ENCLOSURE 2

ATTACHMENT 1

"Test and Analysis Report, Quad Cities New Design Steam Dryer, Dryer #1 Experimental Modal Analysis and Correlation with Finite Element Results," GENE-0000-0039-5860-01-NP, Revision 1, Non-Proprietary, dated May 2005

GE Nuclear Energy

General Electric Company
1989 Little Orchard Street, San Jose, CA 95125

GENE-0000-0039-5860-01-NP
Class I
Revision 1
DRF-0000-0039-5860
May 2005

TEST AND ANALYSIS REPORT
QUAD CITIES NEW DESIGN STEAM DRYER
DRYER #1 EXPERIMENTAL MODAL ANALYSIS AND CORRELATION WITH FINITE ELEMENT RESULTS

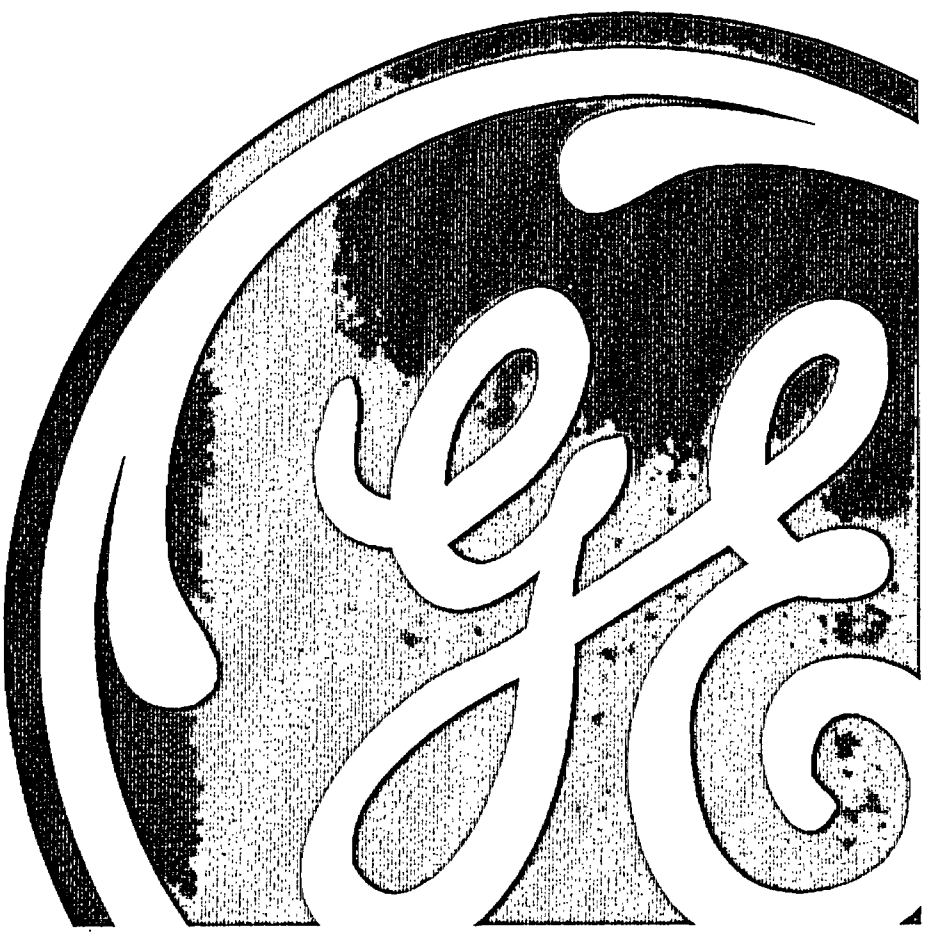

IMPORTANT NOTICE REGARDING CONTENTS OF THIS REPORT

Please Read Carefully

The only undertakings of the General Electric Company (GE) respecting information in this document are contained in the contract between the company receiving this document and GE. Nothing contained in this document shall be construed as changing the applicable contract. The use of this information by anyone other than a customer authorized by GE to have this document, or for any purpose other than that for which it is intended, is not authorized. With respect to any unauthorized use, GE makes no representation or warranty, and assumes no liability as to the completeness, accuracy or usefulness of the information contained in this document, or that its use may not infringe privately owned rights.

Test and Analysis Report
Quad Cities New Design Steam Dryer
Dryer #1 Experimental Modal Analysis and Correlation with Finite Element Results

Table of Contents

List of Tables

List of Figures

Acronyms

BWR	.....	Boiling Water Reactor
DAS	.....	Data Acquisition System
EMA	.....	Experimental Modal Analysis
EPU	.....	Extended Power Uprate
FE	.....	Finite Element
FEA	.....	Finite Element Analysis
FRF	.....	Frequency Response Function
GE	.....	General Electric
GENE	.....	General Electric Nuclear Energy
MAC	.....	Modal Assurance Criterion
MPT	.....	Mode Pair Table
NPT	.....	Node Pair Table
ODS	.....	Operational Deflection Shape
OLTP	.....	Original Licensed Thermal Power
QC1	.....	Quad Cities Unit 1
QC2	.....	Quad Cities Unit 2
RPV	.....	Reactor Pressure Vessel

1.0 Executive Summary

An experimental modal analysis was performed on new design Dryer #1, the instrumented dryer intended for Quad Cities Unit #2 (QC2), and the results were compared to finite element analysis results on a frequency basis and on a mode shape basis. The finite element analysis included a modal analysis and, using those modes from the modal analysis, a mode superposition to obtain FRFs that match the input and response points of the test data. The test results showed many similarities to the finite element results. In terms of frequencies, the trend is that the finite element model frequencies are generally in good agreement with the test frequencies. For example, the first dominant mode of the 90° skirt panel is at [[ ]] in the finite element analysis and at [[ ]] in the test results, a difference of 2.4%. The 270° skirt panel, the 90° hood and the 270° hood all had frequency differences between experimental and analytical results of less than 10% for their lowest frequency dominant modes. In terms of FRF comparisons, the various components examined showed generally good agreement in trends and levels between summation FRFs for test and FE for that specific component.

As expected, the test frequency versus finite element frequency agreement decreased as frequency increased and the modes increased in complexity. The largest potential discrepancy seen between the model and the test is the 90° skirt panel with a significant test frequency being at [[ ]] and the finite element model frequencies at [[ ]] for a vertical 2nd panel bending mode and near [[ ]] for a lateral 2nd panel bending mode. There are several explanations for this discrepancy; however, with the number of sensors on this panel and their locations, a conclusive explanation cannot be provided. The 270° skirt panel and the 90° and 270° hoods showed better agreement for similar frequencies.

The decrease in test versus finite element agreement as frequency increases is expected because, as the mode shapes become more complex with higher frequency, the finite element model results become more sensitive to several parameters such as boundary condition details, element type and number of elements. The boundary conditions of the individual plates, the welds to other plates and beams, are not explicitly modeled in the finite element

model. The wavelengths of the higher modes are shorter so more elements are needed to accurately represent the shapes; however, increasing the number of elements prohibitively increases computation error and adds to round-off error accumulation. The lower skirt super element, which includes hydrodynamic effects of the water on the skirt up to Low Water Level (LWL), may have some effect on the higher mode frequencies and test versus finite element differences as well.

Also, some of the perceived difference for higher frequency modes may be that too few transducers were used in the experimental modal analysis to characterize the mode shape well. The 90° skirt panel is an example where the number of transducers and their location do not appear to allow adequate resolution of some modes whose frequencies appear significantly in the frequency response measurements. Time constraints imposed upon the Dryer #1 experimental modal analysis prevented more locations from being measured. As of the writing of this revision, changes were implemented in the Dryer #2 test plan to add locations to specific components and to reduce the number of conditions (water levels) for testing so that both the time constraint condition and the need for better spatial resolution of the measurement locations are satisfied.

In addition to determining the natural frequencies and mode shapes, the hammer test responses are used to experimentally determine damping values on the skirt and hood at low water level. The purpose of the experimentally determined damping values was to validate the damping values used in the stress prediction analyses. The damping measurement results showed a range of damping values which form a technical basis for arriving at appropriate damping values to be used for structural response analyses.

From the above discussion on the good agreement of the first mode frequency comparisons and the reasonable agreement in the higher mode frequencies, it is concluded that the impact hammer test results verify that the finite element model used for dryer design calculations is sufficiently dynamically similar to the as-built dryer for engineering purposes. In addition the impact hammer test results also show that the [[ ]] value used in the stress prediction analyses are realistic and adequately conservative.

2.0 Scope

This document summarizes the experimental modal analysis and correlation with finite element results performed to compare the finite element model of the new design steam dryer with the actual production Dryer #1. The experimental modal analysis and the finite element analysis were conducted during early April 2005. The following items are included in this document:

1. Description of the testing performed
2. Presentation of experimental data
3. Description of the finite element analysis
4. Comparison of experimental results with finite element results

3.0 Background

This section provides background information intended to help the reader understand the events that precipitated this program.

The original design BWR steam dryers functioned acceptably at Original Licensed Thermal Power (OLTP) for many years. In response to some cracking of original design and modified original design BWR steam dryers when operation shifted to Extended Power Uprate (EPU), GENE has initiated a program to develop a new design of BWR steam dryer with the design intent of being able to survive loads imposed by EPU. As this design was substantially different from the original design, experimental correlation measurements were considered necessary to determine if the finite element analysis used to predict stresses at EPU with its higher loads correlated to actual hardware fabricated according to the new design. Figure 1 is a depiction of the finite element model for the new dryer design, and Figures 2 and 3 are pictures of the actual unit undergoing final assembly.

4.0 Purpose

The testing and analysis described in this document were defined to accomplish the following main objective:

- Determine if the lowest or first dominant frequencies of major components of the new design steam dryer are within 10% of the frequencies predicted by finite element analysis for the dryer configuration at low water level

The specific purpose of the testing, the experimental modal analysis, is as stated in Reference 1, Steam Dryer Hammer Test Specification, GE 26A6380, Revision 1:

- To identify the as-built frequencies and mode shapes of the dryer's key components at ambient conditions.

These as-built frequencies and mode shapes are to be compared with mode shapes, frequencies and FRFs generated from the finite element model of the dryer.

The program has several side objectives as well:

1. To experimentally measure damping values on the skirt and hood at low water level to validate assumptions used in the stress prediction analyses
2. To recommend areas for investigation of differences between model and as-built hardware
3. To recommend areas of improvement of the finite element model to more closely match the as-built hardware

5.0 Experimental Setup

This section describes the test configuration and environment, identifies the instrumentation and data acquisition equipment used, and identifies the sensor locations. The setup and testing follows the requirements outlined in Reference 1, Steam Dryer Hammer Test Specification, GE 26A6380, Revision 1.

5.1 Test Configuration

Steam Dryer #1, the first dryer with the new design, was tested at J.T. Cullen in Fulton, Illinois, a fabrication facility that served as the location for final assembly, installation of the final modifications and installation of the permanent sensors. For the experimental modal test, the steam dryer was supported in a water tank by 4 tripods with extensions that fit into its main support lug sockets. These tripods were welded to metal plates which were bolted to the concrete floor of the fabrication shop. One item to note is that, partway through the testing, the dryer was removed from its supports and transferred to another location for laser dimensional measurements. When it was removed, 2 of the supports had to be detached where they were welded at the floor. When it was returned to its supports, a third support had to be detached from its weld at the floor to align the dryer properly. Data taken before and after this move indicates that some of the low frequency (below 10 Hz) suspension modes were not at exactly the same frequency before and after this move, making the effort to match the actual support stiffness in the FE model more difficult. Figure 4 is a picture of one of the support tripods, and Figure 5 is a close-in picture of the support/dryer connection. A circular tank with a liner was used to hold water for the testing with water. The tank's inner diameter replicated the inner diameter of the reactor pressure vessel (RPV) at the plant to attempt to match the hydrostatic loading at the plant. Testing was performed at 4 different water levels:

1. Dry – no water

2. LWL – Low Water Level – water up to 32.5 inches above the bottom of the bottom flange of the dryer.
3. NWL – Normal Water Level – water up to 36.5 inches above the bottom of the bottom flange of the dryer.
4. HWL – High Water Level – water up to 40.5 inches above the bottom of the bottom flange of the dryer.

All testing was performed at ambient conditions at the test site, with the temperature ranging from 60° F to 75° F

5.2 Data Acquisition System and Instrumentation

The following instrumentation was used to perform the experimental modal analysis and the static test:

1. PCB Model 356A22, 356B08 and 356A15 triaxial accelerometers, and Model 333B30, 333A32, 333B32 and 352C43 single-axis accelerometers

2. PCB Model 086D50 Impact Hammer - after preliminary measurements, the softest hammer tip was selected. Figures 6, 7 and 8 are comparisons of the softest tip with the medium tip. The softest tip provides better low frequency results than the medium tip. The low frequency portion of the FRF is cleaner as seen in the middle plot in Figures 6, 7 and 8, and the low frequency portion of the coherence, the lower plot in Figure 6, 7 and 8, has a higher value with the softest tip. At the start of testing on Dryer #1, it was believed that obtaining very good low frequency data was more important than extending the frequency range of the results; however, subsequent review and discussion of the results produced a decision to use the medium tip for Dryer #2.

3. Vishay Micro-Measurements CEA-06-125UR-350 Strain Gages

4. Omega LC304-5K Load Cell

The following equipment was used to record and analyze the test data:

1. A 116 channel LMS SCADAS III dynamic signal analyzer (2 SCADAS III Model 316 front ends in a Master-Slave configuration) with PQA and PQFA modules was used to provide ICP power to and receive the signal from all of the ICP sensors. For the strain gage measurements, PQBA modules were used in the SCADAS 316 to provide bridge completion and signal conditioning. The system was controlled by a personal computer using LMS Test.Lab 5A software, specifically the Modal Impact, Modal Analysis and Spectral Acquisition modules of software.

5.3 Sensor Locations

The following items detail the contents of Figures 9 through 39 which are pictures that identify the input and response locations used for the experimental modal analysis and static load test.

- Figures 9 through 17 are the 90° hood
- Figures 18 through 25 are the 270° hood
- The 0° vertical side locations are shown in Figures 26 through 32
- The180° vertical side locations are shown in Figures 33 through 34
- Figures 35 and 36 contain the test wireframe for the 0° vertical side locations and the180° vertical side locations
- Figures 37 and 38 depict the impact locations and the accelerometer and strain response locations for the 90° skirt panel and the 270° skirt panel

5.4 Frequency Response Function Measurement Settings

The signal processing parameters used for data acquisition were the following:

- 5 to 10 averages (1 average for the time domain damping measurements) (Attachment C is a comparison of results from 5 averages and 20 averages for one measurement location on Dryer #2 to show that using 5 to 10 averages is

adequate, and the GE Hammer Test Specification, Reference 2, specifies 3 or more)

- Force window of 5% to 20% on the input (Uniform window used for damping measurements)
- Exponential window of 3% to 20% on the responses (Uniform window used for damping measurements)
- Effective Frequency bandwidth of 400 Hz (actual bandwidth setting 512 Hz, sampling frequency of 1024 Hz)
- 4096 Spectral lines (0.125 Hz resolution/8.0 second time length)
- 0.1 second pretrigger on the hammer input

For the measurements, the following results were saved:

- Frequency Response Function
- Coherence
- Input Autopower
- Response Autopowers
- Time Record (for time domain damping measurements only)

5.5 Test Documentation

Attachment D contains the channel assignment data sheets as referred to in the GE Hammer Test Specification. Attachment E contains the test log sheets. The test log sheets have been rewritten from the original LMS test log sheets to match the GE format and to clean them up.

6.0 Test Results

This section presents a subset of the test results. It covers the damping results based on experimental measurements and other experimental results on components that are not compared to FE results on a component basis. Additional test results that are correlated to FE results are presented in **Section 8.0, Correlation of Test Results and Finite Element Results.**

6.1 Skirt Damping Measurement Results

Specific measurements were performed to measure the damping on the 90° skirt panel and on the 270° skirt panel at low water level. Acceleration and strain responses were acquired on these panels in response to impacts. Figures 38 and 39 show the impact and response locations for the 90° skirt panel and on the 270° skirt panel, respectively, for the damping measurements.

Damping was calculated in the frequency domain using modal curve-fitting methods on individual FRF measurements and on all of the FRF measurements for the specific component and using the half power bandwidth method or equivalent methods with different "dB down" values and in the time domain using the log decrement method. Reference 2, SAE Recommended Practice J1637, contains the calculations for the equivalent methods to the half power bandwidth method, and Reference 3 provides a discussion of the modal curve-fitting method used for the individual FRFs and for the whole component analysis.
The damping results on the skirt are presented in Table 1.

Table 1: Dryer #1 Skirt Damping Results at Low Water Level

[[

]]

The damping in terms of percent critical damping ranged from [[ ]] on the 90° skirt panel, with the higher frequencies generally showing less damping. The 270° skirt panel showed a similar trend, with a range of [[ ]] In general, the strain gages showed slightly higher damping levels for the same mode than the accelerometers.

6.2 Hood Damping Measurement Results

Specific measurements were performed to measure the damping on the 90° hood and on the 270° hood at low water level. Acceleration was acquired on these panels in response to impacts. Figures 11 through 15 and Figures 20 through 25 show the impact and response locations for damping measurements on the 90° hood and on the 270° hood, respectively.

Damping was calculated in the frequency domain using modal curve-fitting methods on individual FRF measurements and on all of the FRF measurements for the specific component and using the half power bandwidth method or equivalent methods with different "dB down" values. Table 2 contains the damping values for the hoods.

Table 2: Dryer #1 Hood Damping Results at Low Water Level

[[

]]

The hood panels generally showed less damping than the skirt panels. Percent of critical damping values ranged from [[ ]] on the 90° hood and from [[ ]]on the 270° hood. Again, damping decreased as frequency increased.

6.4 Discussion of Damping Results

Several questions arise in review of damping results. One question is, "Why does the damping decrease with frequency?"

1. The input force decreased as frequency increased. Quite often, there is a relationship between input force and measured damping, with damping increasing as input force

increases, so possibly in this case the decrease in force versus frequency is also affecting the decrease in damping versus frequency

2. The loading of the water on the lower skirt panel has a greater damping effect at low frequency than high frequency

A brief literature review produced no results that appear to be immediately relevant to a large welded structure such as the dryer.

Another question concerned the increase in damping from accelerometer to strain results. Again, 2 possibilities are present but no conclusive determination has been made:

1. The strain gages were at the panel edges, greater than 1 inch from the weld but closer than 3 inches, while the accelerometers were in the middle of the panels. It is believed that these locations could show more damping than the accelerometer locations
2. The strain gage is a displacement-based device while the accelerometer is acceleration-based. There is some belief that this difference is causing a slight increase in damping estimates from strain versus those from acceleration.

Further review of both damping versus frequency and damping from strain versus damping from acceleration will be performed using Dryer #2 data when it is available.

6.5 Dryer Top Experimental Results

This section contains experimental results from the dryer top as well as a very limited number of the points on the inner hood and perforated plates. No specific correlation exercise was performed for the dryer top so only the experimental results for modes from curve-fitting up to 100 Hz are presented here.

Table 3: Dryer #1 Top Experimental Frequencies

Mode Number	Test Data Frequency	Percent Critical Damping
Mode 1	[[	
Mode 2		
Mode 3		
Mode 4		
Mode 5		
Mode 6		
Mode 7		
Mode 8		
Mode 9		
Mode 10		
Mode 11		
Mode 12		
Mode 13		
Mode 14		
Mode 15		
Mode 16		
Mode 17		
Mode 18		
Mode 19		
Mode 21		
Mode 22		
Mode 25		
Mode 26		
Mode 28		
Mode 29		
Mode 30		
Mode 32		]]

Table 3 contains significant frequencies for the dryer top below 100 Hz, and Figure 40 contains the summation FRF for the dryer top measurements. The summation FRF is an average of the FRFs in all 3 directions for the included points unless noted. Some of the

summation FRFs presented in this report will only be the measurements perpendicular to the surface and will be noted as such

[[

]]

6.6 0° Vertical Side Experimental Results

As with the dryer top, no specific correlation to finite element results was performed for the 0° vertical side. Figure 41 is the summation FRF for the 0° vertical side, and Table 4 on the next page contains significant frequencies for this component below 94 Hz. The 180° vertical side is omitted because there was not a specific impact point on that side due to lack of access.

[[

]]

Table 4: Dryer #1 0° Vertical Side Experimental Frequencies

Mode Number	Test Data Frequency	Percent Critical Damping
Mode 5	[[	
Mode 6		
Mode 7		
Mode 8		
Mode 9		
Mode 10		
Mode 11		
Mode 12		
Mode 13		
Mode 15		
Mode 17		
Mode 18		
Mode 20		
Mode 21		
Mode 22		
Mode 23		
Mode 24		
Mode 25		
Mode 26		
Mode 27		
Mode 28		
Mode 29		
Mode 30		
Mode 31		
Mode 32		
Mode 33		
Mode 34		
Mode 35		
Mode 36		
Mode 38		
Mode 39		
Mode 40		
Mode 41		
Mode 42		
Mode 46		
Mode 49		
Mode 50		
Mode 51		
Mode 52		
Mode 53		
Mode 54		
Mode 55		
Mode 56		]]

7.0 Correlation

This section discusses the process of using finite element model results to correlate with experimental test results.

7.1 Procedure

The goal of the correlation is to determine the differences between the FE model and the test object and to determine the sensitive spots of the FE model. Afterwards, one can improve the correlation, focusing on those hot spots, and finally obtain a model that is more realistic than the previous one.

The correlation procedure contains the following steps:

- Geometric correlation: Definition of a relationship between the units, the coordinate systems and the measuring points of the TEST model on one hand, and the units, the coordinate systems and the nodes of the FE model on the other hand.
- Modal correlation: Comparison of the experimental mode shapes and the FE mode shapes, based on wireframe animations and MAC (modal assurance criterion) calculations.
- Correlation of the transfer functions: Comparison of the measured FRFs and the ones calculated directly or synthesized from the FE mode shapes.

The calculations of the FE mode shapes and FRFs have been done here with ANSYS 8.1. The correlation has mainly been done in LMS/LINK and Test.Lab.

7.2 Geometric Correlation

This phase ensures the compatibility between the measured and the calculated data. It includes the following steps:

1. Definition of rational entities/groups in the model, grouping nodes that have common properties or are part of the same panel for example. Those entities are called components.

2. Definition of pairs between TEST measuring points and FE nodes. These pairs are stored in a node pair table (NPT). This table allows the automatic projection of the TEST geometry on the FE geometry.
3. Compatibility between the global and local coordinate systems. This information is also contained in the node pair table and ensures a proper projection of the TEST geometry on the FE geometry.
4. Transformation of the TEST data (modes, FRFs, wireframes) to the verification system (FE model), in order to make the comparison easier.

All these steps were done in LMS/LINK.

7.3 Modal Correlation

The dynamic behavior of a structure, at least in the low frequency range, is best described by its normal modes. From experimental normal analysis, the modes of the structural components are known with their shapes, frequencies, and modal damping.

For the FE model, shapes and frequencies of normal modes are calculated in ANSYS 8.1 (analysis ANTYPE, 2). For the test results, the general process has been to calculate the complex modes first, review those modes, and then use the same poles to calculate the normal modes for comparison with FE results.

Experimental modes can be directly compared to FE modes by using the wireframe animations from both Test and FE. Using this technique, important conclusions can be drawn regarding parts that are not well modeled in the FE.

After the first mode extraction for example, four grounded springs were added to the model as boundary condition. These grounded springs (COMBIN14) were fixed to the dryer ring in the 4 support points. This was intended to model as simply as possible the support beams used in the test rig that support the dryer. This was necessary to be able to extract the suspension modes and model the influence that the supports have on the rest of the structure as there was concern that the support stiffness influenced some of the lower frequency flexible modes of the dryer.

Of course, FE modes can also be visualized with the entire model, and not only the wireframe geometry. This way, one can easily understand the real nature of the modes, which is not always obvious with wireframe animations.

Another tool to judge modal correlation is the Modal Assurance Criterion (MAC). It expresses the nature of the relationship between two sets of vectors. For each pair of modes compared, it is calculated from the vectors of each degree of freedom considered in the correlation model. Mathematically, the MAC is defined as

$$MAC_{rr'}=\frac{\left|\{\psi_r^{test}\}\{\psi_{r'}^{FE}\}^*\right|^2}{\left(\{\psi_r^{test}\}\{\psi_r^{test}\}^*\right)\left(\{\psi_{r'}^{FE}\}\{\psi_{r'}^{FE}\}^*\right)}$$

where $\left(\Psi_r^{test}\right)$ is a modal vector from test and $\left(\Psi_{r'}^{FE}\right)$ is a modal vector from the finite element solution. These modal vectors each represent a single frequency and contain the common degrees of freedom between the test and the FE, in this case either on a global basis or on a component basis. For identical modes, the MAC is 1. For linearly independent mode shapes, the MAC is 0. As the MAC formulation includes a quadratic term, small or local deviations between Test and FE will result in considerably lowered MAC values.

Unfortunately, the FE modal density at low frequency is already very high for the dryer. And too many local effects are already present at the very low frequencies (this is a direct result of the low stiffness of the perforated inner panels of the dryer). As a result, the global modes are mixed/lost among many local modes. For example here, in the 200 first FE modes, only 10 had global characteristics; all the others were 1st, 2nd and 3rd bending modes of the inner perforated panels.

On the other hand, the low number of measuring points on a region makes it impossible to capture those local modes in the experimental TEST modal analysis.

As result, one TEST mode corresponds to many FE modes, global, local or mixed. A one-to-one TEST-FE mode comparison is thus very difficult, and makes it almost impossible to draw any conclusion of the MAC analysis.

The MAC analysis was still used, but generally only after other methods discussed in the next sections had narrowed down the frequency range to be examined.

7.4 FRF Correlation

Normal modes are an efficient representation of the dynamic behavior of a structure, but only useful for correlation as long as the modes are not combining too many local effects. As mentioned above, even at low frequency, there are many local modes, making it virtually impossible to combine the same local effects in one mode of the FE model, as can be observed in the test model. In reality, different local effects get shifted to different frequencies, making it impossible to find the same combination of the same local effects in test and FE. As long as the same local effects occur at approximately the same frequency, a good dynamic correlation is obtained, even if this is not visible in a MAC matrix.

Another way thus to compare dynamic behavior of two models is looking at frequency response functions (FRFs). They can be evaluated over the whole frequency range of interest. In an FRF, the (acceleration) response of one point is plotted as function of a unit (force) input in another point. Modes can be found as peaks in an FRF, and the higher the modal damping, the lower and broader the peak will be.

For checking correlation, the synthesized FE FRFs are compared with the corresponding measured test FRFs. More interesting than the exact amplitude is the general shape of a FRF. A good correlation means that important peaks from the test should be found in the synthesized FRFs at a similar frequency, and the general amplitude of the FE and test FRFs are similar.

A FRF can be calculated in ANSYS with the harmonic response analysis (ANTYPE, HARMIC). The idea is to impose a unitary force in one DOF of the hitting points and

calculate the frequency response (displacements or accelerations) in all the DOFs of all the other points. The obtained response functions can then effectively been seen as displacements or accelerations per unit input force.

Three methods of solution are available in ANSYS to calculate FRFs with the harmonic response analysis:

1. Full (HROPT, FULL)
   This method solves the general equation of motion of a structural system transposed in frequency domain directly.

2. Reduced (HROPT, REDUC)
   The reduced solution method uses reduced structure matrices to solve the equation of motion. This method runs faster than the full harmonic response by several orders of magnitudes, because the technique of matrix reduction is used so that the matrix used to represent the system is reduced to the essential DOFs required to characterize the response of the system.

3. Mode superposition (HROPT, MSUP)
   The mode superposition method uses the natural frequencies and mode shapes from the modal analysis (ANTYPE, MODAL) to compute the dynamic response to steady harmonic excitation. It converts the equation of motion in its modal form. The advantage of this method is that the computationally expensive matrix algebra can be calculated inexpensively in modal coordinates. The individual modal responses are then superimposed to obtain the actual response.

The Full method is very memory and time-consuming and was not used in this project. The Mode Superposition technique was preferred here. This method has as an advantage that the mode shapes only have to be calculated once and can be re-used to calculate FRFs for different input points. On the other hand, the reduced and full harmonic methods have to be repeated for each hitting point.

7.5 Changes to As-received model

Several changes were made to the model after it was received from GE to more closely replicate the test conditions.

- Elastic modulus and damping changed to ambient conditions from reactor conditions (the lower skirt super element with its loading by water was left unchanged)
- Removal of pressure loading (a pressure loading from reactor condtions)
- Addition of grounded springs instead of perfectly rigid constraints at the support locations (the dryer as tested was supported on stands that exhibited flexibility as compared to the completely rigid FE constraints. A complete iteration of these springs to match the test results was not performed, and the dryer move for laser dimensional measurements caused the final sets of data to have slightly different support stiffnesses.)

8.0 Correlation of Test Results and FE Results

This section presents comparisons between test results and finite element analysis results on several levels:

- Global
- Skirt Component
- 90° Hood Component
- 270° Hood Component

The comparisons are presented as comparisons of frequencies, comparison of test FRFs to FE FRFs, comparison of local mode shapes and comparison of global mode shapes. Comparison started on a global level and moved to a component level due to the many closely spaced modes of some of the dryer components in the finite element model. Because of the modal density, many of the test modes appear similar to numerous FE modes, making it very difficult to find a single corresponding mode. Correlation on a component basis was performed by observing significant peaks in the summation FRF and some individual FRFs

of the component to narrow down the frequency range for searching the FE modes and then reviewing the mode shape animations and MAC matrices for the test and FE components. Also, for the skirt and both hoods, 2 relatively widely spaced peaks in the frequency domain were examined. After that review, the other components were added to the mode shape to observe the global mode that the component mode was related to.

8.1 Global Comparison

The results from the experimental modal and the finite element analyses have been compared on a global level. There are similar modes under 10 Hz that are directly controlled by the modeling of the supports. The stiffness of the support springs is still too low as the suspension modes of the FE model are at a lower frequency than those of the test results for similar modes under 10 Hz. For this study, it was decided to stop the iterative adjustment of the support springs as its effect on the component modes was expected to be minimal, but this adjustment is still an area for potential improvement.

The first significant global flexible mode is found at [[ ]], a mode in which the hoods appear to slide laterally out of phase with each other with what appears to be a twist or rotation of the skirt and ring. The finite element counterpart to this mode ended up at [[ ]] with the grounded springs used at the support locations. This frequency difference could probably be reduced with further adjustment of the grounded spring supports; however, as mentioned above, it was decided to stop iterating the FE grounded springs to match the test.

After the initial attempt at the global comparison, the focus shifted to a component basis and sometimes expanded to the global modes related to those specific component modes.

8.2 Skirt Component Comparison

The skirt was the first component to be analyzed on a component basis. Table 5 contains frequencies from the test data analysis and a limited number of frequencies from the finite element results.

Table 5: Dryer #1 Skirt Experimental Frequencies

[[

]]

Figure 42 contains the skirt summation FRF, a comparison between test and FE results. Figures 43 and 44 contain individual FRF comparisons between test and FE for the points measured on the 90° skirt panel, while Figure 45 contains additional results for points located off of the panel centerline. Figures 46 through 48 are similar results for the 270° panel. Figure 49 compares the 90° skirt panel and the 270° skirt panel test results.

The first mode of the 90° skirt panels appears to be within 10% of the finite element prediction (first panel mode at [[ ]] for FE). Figure 50 is the mode shape comparison of these modes.

The first mode of the 270° skirt panel appears to be in the [[ ]] range when the damping measurement FRFs are reviewed along with the modal information. For the FE

results, the range of frequencies is [[
]].

There are several more complex skirt modes in the [[ ]] frequency range as well. In terms of visual comparison of modes based on a peak in the FE summation FRF, the test mode at [[ ]] as shown in Figure 51.

For the panel modes, the 90° skirt panel appears to have an intermediate mode (not clearly 2nd bending, more of a cantilever) in the test results in the [[ ]] range where the lower point is active normal to the panel surface, but the upper point is stationary.

In FE there is clearly a 2nd panel mode of the 90° skirt panel at [[ ]] This 2nd panel mode is most clearly similar to test frequencies of [[ ]] visually but most clearly similar to the [[ ]] test mode in the FRF comparison as shown in Figures 43 and 44. Figures 52 and 53 contain the mode shape comparisons for both test frequencies. Objections have been raised to this comparison because the FE results show a lateral bending mode of this panel at approximately [[ ]] and the test sensor locations would be at or near the node line for this mode; however the FRFs from both the modal and the damping measurements in Figures 43 and 44 show the clearest 2nd peak of the panel FRFs at [[ ]] Figure 45 contains additional FRFs from points not on the centerline of the 90° skirt panel compared to the points on the centerline of the 90° skirt panel. In summary, there are several explanations for the appearance of the FRF and mode shapes but none of the explanations are conclusive with the data available for the 90° skirt panel:

1. The sensors are picking up the 2nd lateral panel bending mode even though the centerline sensors should be insensitive to this mode
2. The sensors are observing the 2nd vertical panel bending mode, and this mode is 20% higher in frequency than predicted by FE
3. The 2nd lateral panel bending mode is geometrically rotated. The 90° skirt panel is the last panel welded into the structure. It is believed that it is very sensitive to the

weld sequence. Preliminary results from Dryer #2 with a larger number of sensors on this panel indicate that the 2nd lateral panel mode is not strictly side-to-side but rather upper-left to lower-right when observed by an observer facing the panel exterior. This explanation coincides to some degree with explanation 1. as well.

Also, a comparison of the FRFs from the damping measurements with those from the 270° skirt panel in Figure 49 shows the 2nd major mode of the 270° skirt panel near [[

]]

Based on the apparent discrepancy in frequency between test and FE results for the 90° skirt panel, a skirt sub-model study was performed to determine if the instrumentation pads, conduit and clamps affected this mode on the 90° skirt panel. The 90° skirt panel had this instrumentation while the 270° skirt panel did not. The next section describes this study and its results.

8.2.1 Skirt Sub-Model Study

A study of the skirt was performed to determine the effect of the instrumentation pads, clamps and conduit on the frequencies of the modes of the 90° skirt panel. These components were found to have no significant effect on the frequency or shapes of the panel modes of the 90° skirt panel. The frequency difference between base model and model with instrumentation pads, clamps and conduit was [[ ]]or less for all modes examined. Table 6 contains the percentage change for the first 6 modes of the panel.

Details of the skirt sub-model for the study are as follows:

- Use only skirt section for which elements are available (do not use lower skirt super element)
- Constrain so that no displacements are possible at top and bottom of skirt section (full constraint – 3 directions/3 rotations)
- The sub-model frequencies were slightly different than those of the full model but always within 10%

- Instrumentation pads – stitched to skirt
- Conduit modeled as beam elements
- Clamps modeled as rigid connections (no mass addition, only stiffness – conservative assumption – will not reduce frequency)
- Plate thickness remains same from whole model
- Material Properties (reactor properties allowed frequency match to whole model modes more closely)
    - 2.56e6 psi elastic modulus
    - 7.4e-4 slugs/in^3 density
    - Also checked using ambient properties – frequencies shifted up by approximately 4% to 4.5% but did not change effect of instrumentation pads, clamps and conduit

Table 6: Frequency Change after addition of instrumentation to 90° skirt panel

[[

]]

Appendix B contains finite element mode shapes from the Skirt Sub-Model analysis that was used to determine the effect of the instrumentation pads, clamps and conduit.

8.3 90° Hood Component Comparison

The 90° hood test results were compared to finite element predictions. Figure 53 is the summation FRF for all 3 directions for this component – a comparison of test and FE, while Figure 54 is the summation FRF for this component in the X-direction for FE and normal to the surface for test (12.5° Euler angle between the FE and test results). A comparison of Figures 53 and 54 shows that the direction normal to the surface dominates the summation

FRF. As with the other components examined, the [[

]] clearly appears. Table 7 contains the test mode frequencies and comparisons with several FE mode frequencies.

The first flexible mode of the 90° hood appears to be in the [[

]]

Visually these appear similar, but the component summation FRF more readily supports a [[ ]].

For the hood upper frequency range around [[ ]] similar modes emerged in both the visual comparison and the MAC calculation. Figure 57 compares mode shapes at [[

]] solution. Figure 58 is a MAC matrix of this frequency range that shows a cluster of test modes being very similar to a larger cluster of FE modes.

Table 7: Dryer #1 90° Hood Experimental Frequencies

[[

]]

8.4 270° Hood Component Comparison

The 270° hood test results were compared to finite element predictions at frequencies similar to the frequency regions used for the 90° hood. Table 8 contains the significant test modes and frequencies of similar FE modes. As with the other components evaluated the global mode at [[ ]]was present. For the 270° hood, the first flexible mode, although one related to significant skirt activity, appears at [[

]]. Figure 59 compares test and FE summation FRFs, and Figure 60 compares test and summation FRFs for the direction normal to the hood surface for test and in the X-direction for FE. Note that there is an angular difference of 12.5° between the test and FE directions in this case. Individual FRF comparisons between Test and FE are contained in Figures 61 and 62. Figure 63 shows a comparison of component-level mode shapes at [[ ]]while Figure 64 is the global comparison a those frequencies. This difference in frequency is approximately 10% although there is a cluster of [[ ]] is similar to.

As for the 90° hood, the other frequency range of interest for the 270° hood is the [[
]] Figure 65 contains the MAC matrix display around [[
]]results. The [[
]]. It is most similar to a [[ ]], shown in Figure 66 on a component level and Figure 67 on a global level.

Table 8: Dryer #1 270° Hood Experimental Frequencies

[[

]]

A general observation of the summation FRFs for the 270° hood is that the level of the FRF predicted by FE is lower in the [[ ]] This difference can be seen in Figures 59 and 60. The hood in FE may be too stiff or its connections may be too stiff as the general trend of the FE versus test comparison for the hood is that the FE levels are lower than the test levels.

8.5 Additional Observations

This section contains additional observations from reviewing the test results in comparison with the analytical results.

1. When comparing predicted FRFs to experimentally measured FRFs, responses on the ring or skirt from inputs to the hood show the FE levels ranging from similar to too high, indicating that the skirt may not be stiff enough in FE.
2. In many of the animations reviewed, the amplitude of the skirt compared to the amplitude of the hoods in mode shapes in FE is higher than the relative amplitudes for a similar test mode shape. The possibilities for this occurrence are the following:
    a. in FE, the relative stiffness of the hoods is too high with respect to the skirt.
    b. in FE, the mass of the hoods is too high with respect to the skirt.
    c. in FE, the skirt and the hood are too closely coupled and adjustments need to be made to the connections between the hoods, the support ring and the skirt
3. In terms of being a potential area for improvement, the skirt and its connection to the ring ranks as the highest areas because the 90° skirt panel 2nd vertical and lateral panel modes predicted by FE do not match the test results because there is either a frequency difference or a shape/orientation difference and because the FRF and animation trends (cross-FRFs with other components and relative amplitude in FE animations of skirt to other components compared with test animations) show that the skirt may generally not be modeled as stiff enough in the finite element analysis, or its connection to the ring may require review or there may be some aspect of the lower skirt super element affecting it more than desired for this comparison.

9.0 Summary and Conclusions

An experimental modal analysis was performed on new design Dryer #1, the instrumented dryer intended for Quad Cities Unit #2 (QC2), and the results were compared to finite element analysis results on a frequency basis and on a mode shape basis. The finite element analysis included a modal analysis and, using those modes from the modal analysis, a mode superposition to obtain FRFs that match the input and response points of the test data. The test results showed many similarities to the finite element results. In terms of frequencies, the trend is that the [[

]] dominant modes.

As expected, the test frequency versus finite element frequency agreement decreased as frequency increased and the modes increased in complexity. The largest potential discrepancy seen between the model and the test is the 90° skirt panel with a significant test frequency being at [[ ]] for a vertical 2nd panel bending mode and near 70 Hz for a lateral 2nd panel bending mode. There are several explanations for this discrepancy; however, with the number of sensors on this panel and their locations, a conclusive explanation cannot be provided. The 270° skirt panel and the 90° and 270° hoods showed better agreement for similar frequencies. In terms of FRF comparisons, the various components examined showed generally good agreement in trends and levels between summation FRFs for test and FE for that specific component.

The decrease in test versus finite element agreement as frequency increases is expected because, as the mode shapes become more complex with higher frequency, the finite element model results become more sensitive to several parameters such as boundary condition

details, element type and number of elements. The boundary conditions of the individual plates, the welds to other plates and beams, are not explicitly modeled in the finite element model. The wavelengths of the higher modes are shorter so more elements are needed to accurately represent the shapes; however, increasing the number of elements prohibitively increases computation error and adds to round-off error accumulation. The lower skirt super element, which includes hydrodynamic effects of the water on the skirt up to Low Water Level (LWL), may have some effect on the higher mode frequencies and test versus finite element differences as well.

Also, some of the perceived difference for higher frequency modes may be that too few transducers were used in the experimental modal analysis to characterize the mode shape well. The 90° skirt panel is an example where the number of transducers and their location do not appear to allow adequate resolution of some modes whose frequencies appear significantly in the frequency response measurements. Time constraints imposed upon the Dryer #1 experimental modal analysis prevented more locations from being measured. As of the writing of this revision, changes were implemented in the Dryer #2 test plan to add locations to specific components and to reduce the number of conditions (water levels) for testing so that both the time constraint condition and the need for better spatial resolution of the measurement locations are satisfied.

In addition to determining the natural frequencies and mode shapes, the hammer test responses are used to experimentally determine damping values on the skirt and hood at low water level. The purpose of the experimentally determined damping values was to validate the damping values used in the stress prediction analyses. The damping measurement results showed a range of damping values which form a technical basis for arriving at appropriate damping values to be used for structural response analyses.

To summarize:

1. The FE results contain many modes so generally a specific test mode will be similar to a group of FE modes in a specific frequency range
2. Specific lower frequency dominant modes of the skirt and the hoods appear to be similar in frequency and shape between Test and FE
3. FRF comparisons of component summation FRFs showed generally good agreement of levels and trends, with the only major exception being the [[
   ]] of the 270° hood
4. Individual FRFs often showed good agreement of levels and trends. An exception is the 90° skirt panel. It is discussed further in the next item.
5. The 90° skirt panel as installed appears to show the most difference from FE results in its 2nd panel modes. Further work is necessary to determine the source of the differences as initial checks of the model produced no insight. Additional analysis of Dryer #2 results is expected to provide information for this panel.
6. Plans for similar testing on the next dryer will include more detailed measurements/additional locations on the 90° skirt panel and the 270° skirt panel and on both of the hoods.

From the above discussion on the good agreement of the first mode frequency comparisons and the reasonable agreement in the higher mode frequencies, it is concluded that the impact hammer test results verify that the finite element model used for dryer design calculations is sufficiently dynamically similar to the as-built dryer for engineering purposes. In addition the impact hammer test results also show that the [[
]] used in the stress prediction analyses are realistic and adequately conservative.

10.0 References

1. Ramani, Venkat "Steam Dryer Hammer Test Specification." GE 26A6380. GENE. San Jose, CA. April 2005.

2. "Laboratory Measurement of the Composite Vibration Damping Properties of Materials on a Supporting Steel Bar." Recommended Practice J1637, Society of Automotive Engineers. Warrendale, PA. February, 1993.

3. Peeters, Bart; Guillame, Patrick; Van der Auweraer, Herman; Cauberghe, Bart; Verboven, Peter; Leuridan, Jan. "Automotive and Aerospace Applications of the PolyMAX Modal Parameter Estimation Method." Proceedings of International Modal Analysis Conference (IMAC) 22. Dearborn, MI. January, 2004.

Figures

[[

]]

Figure 1: Finite Element Model Representation of Dryer

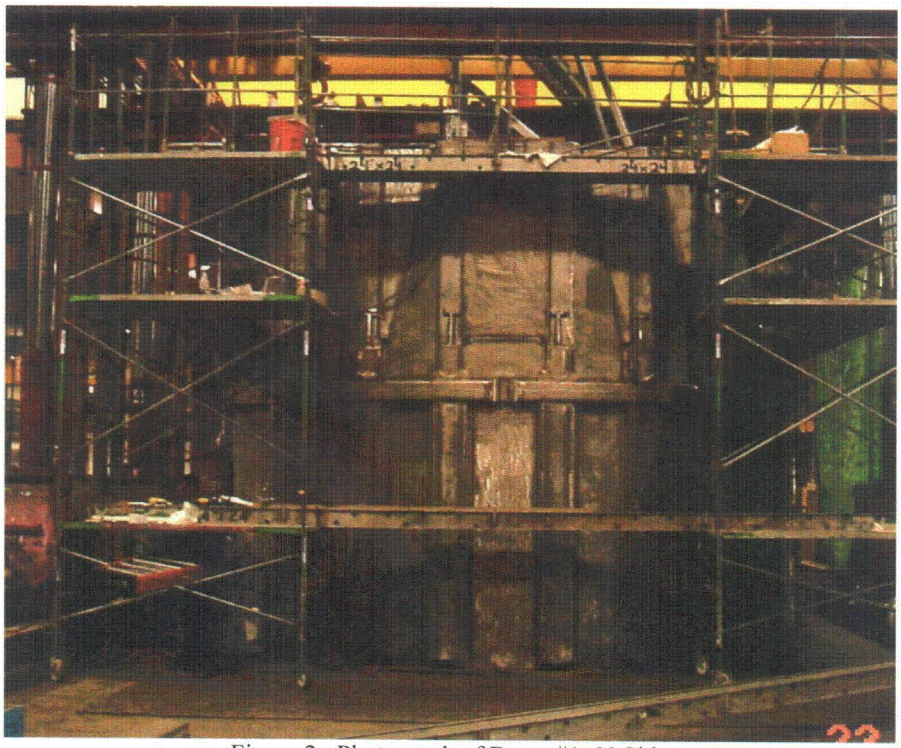

Figure 2: Photograph of Dryer #1, 0° Side

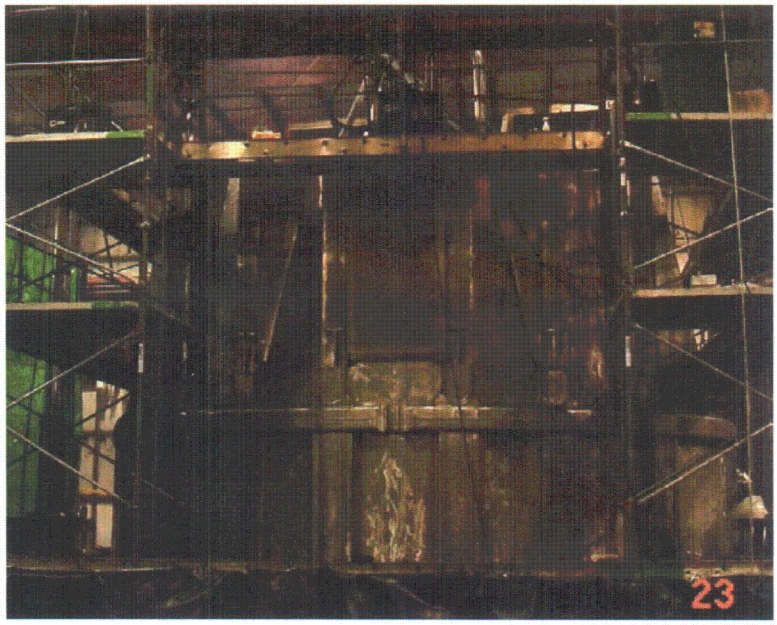

Figure 3: Photograph of Dryer #1, 180° Side

Figure 4: Tripod Supports before Installation

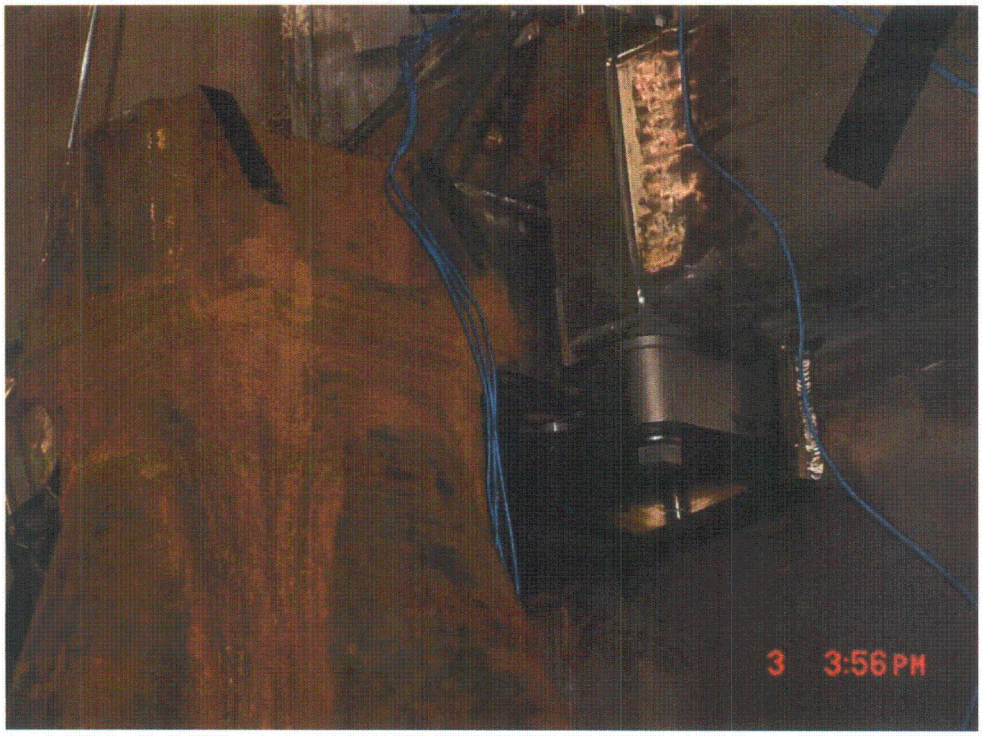

Figure 5: Tripod Support Connection to Dryer

[[

]]

Figure 6: Comparison of Measurements using Hammer Tips of different hardness, Radial Skirt Response to Radial Skirt Impact (Red curve is soft tip, Green curve is medium tip)

[[

]]

Figure 7: Comparison of Measurements using Hammer Tips of different hardness, Vertical Side Response to Skirt Impact (Red curve is soft tip, Green curve is medium tip)

[[

]]

Figure 8: Comparison of Measurements using Hammer Tips of different hardness, 90° Hood Response to Skirt Impact (Red curve is soft tip, Green curve is medium tip)

Figure 9: Full view of 90 degree hood of dryer #1 during measurements.

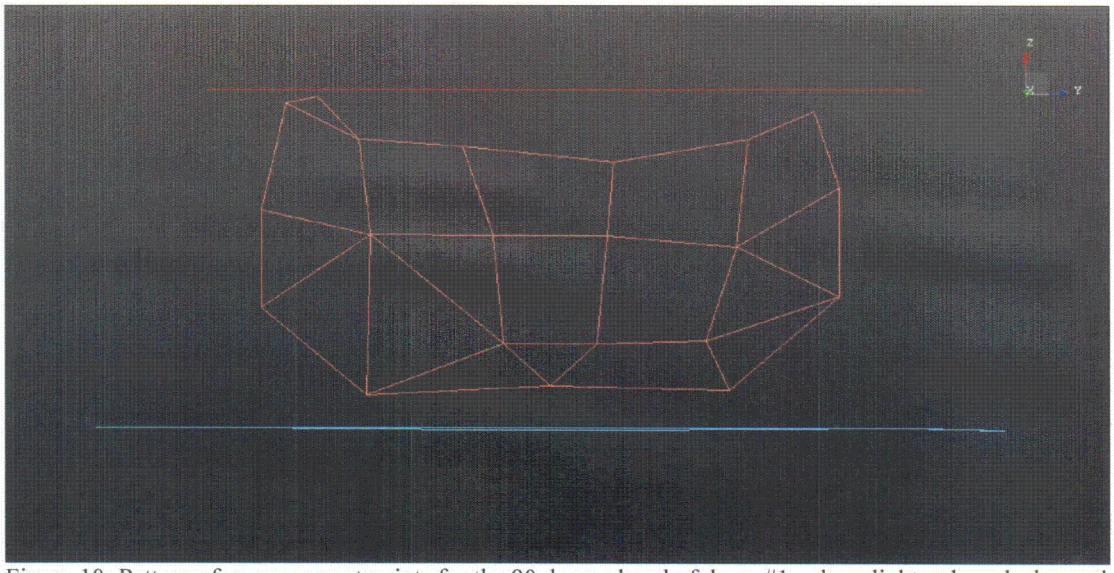

Figure 10: Pattern of measurement points for the 90 degree hood of dryer #1, where light red mesh shows the 90 degree hood response locations, dark red represents the responses on top & aqua represents the responses on the ring.

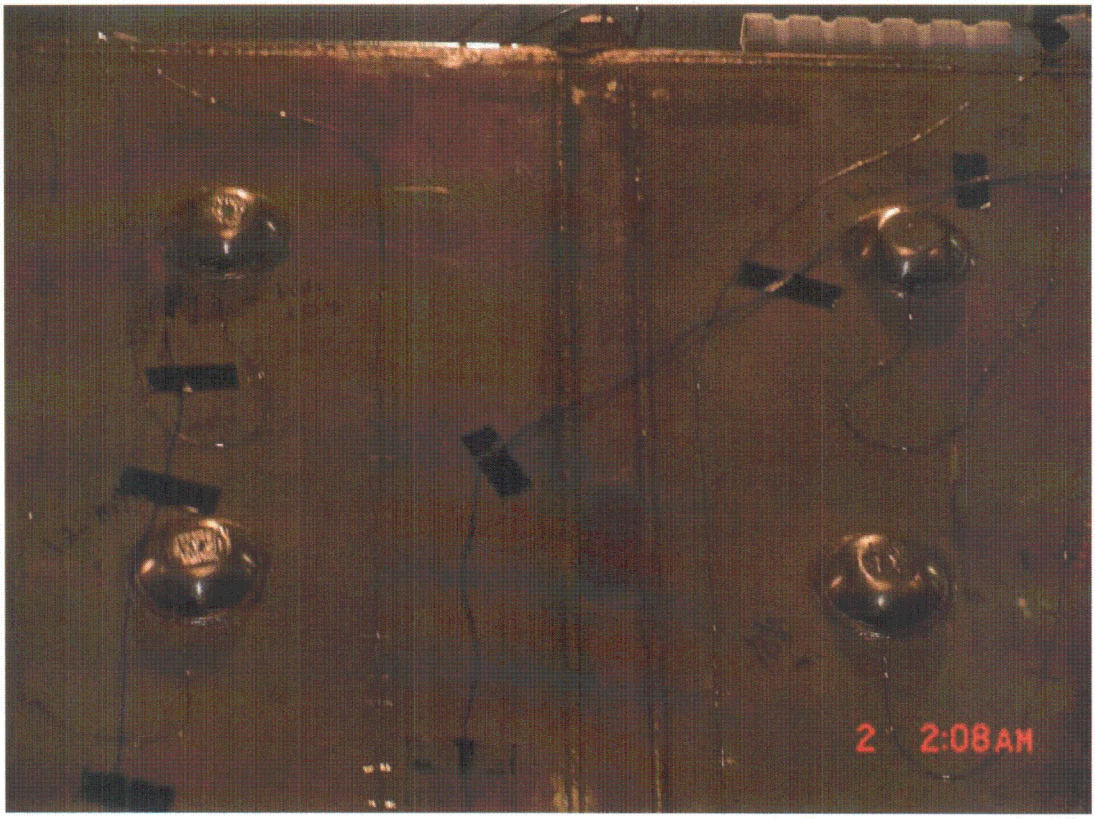

Figure 11: Response locations on upper right corner of 90 degree hood of dryer #1.

Figure 12: Response locations on lower right corner of 90 degree hood of dryer #1.

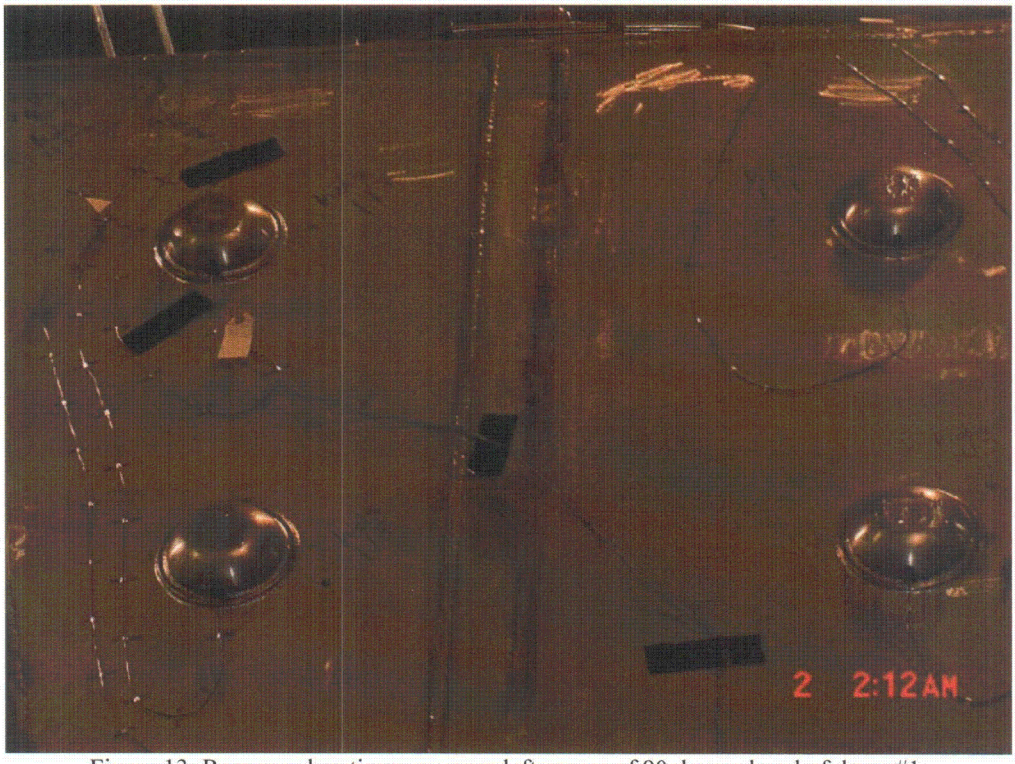

Figure 13: Response locations on upper left corner of 90 degree hood of dryer #1.

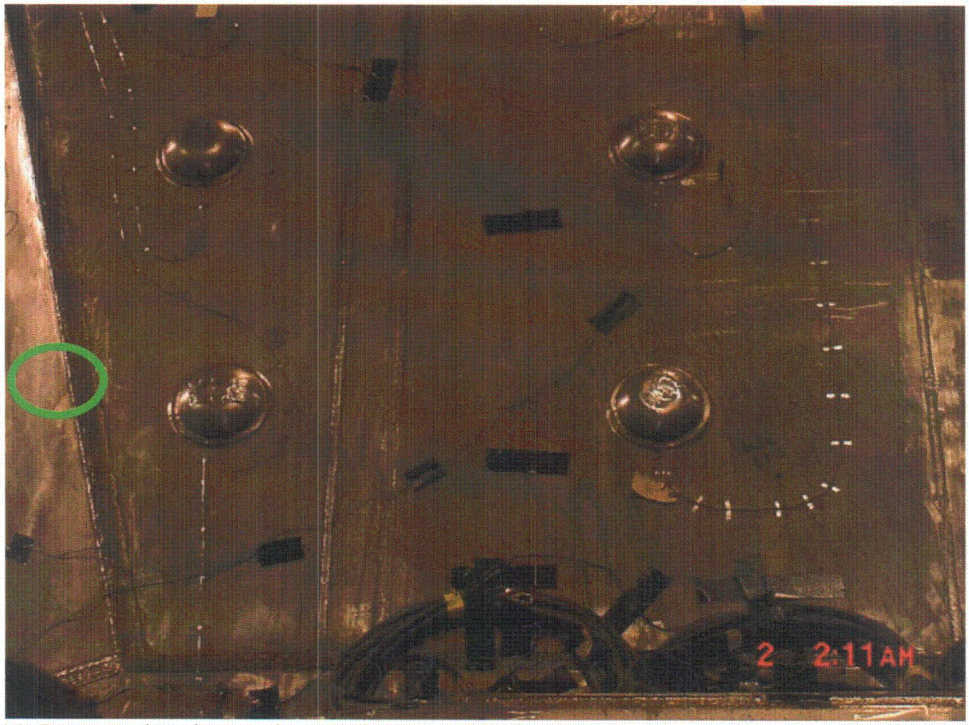

Figure 14: Response locations on lower left corner of 90 degree hood of dryer #1 with green circle indicating input location on 90 degree hood.

Figure 15: Response location on side panel to the right of main panel of 90 degree hood of dryer #1 (at angle w.r.t. main panel).

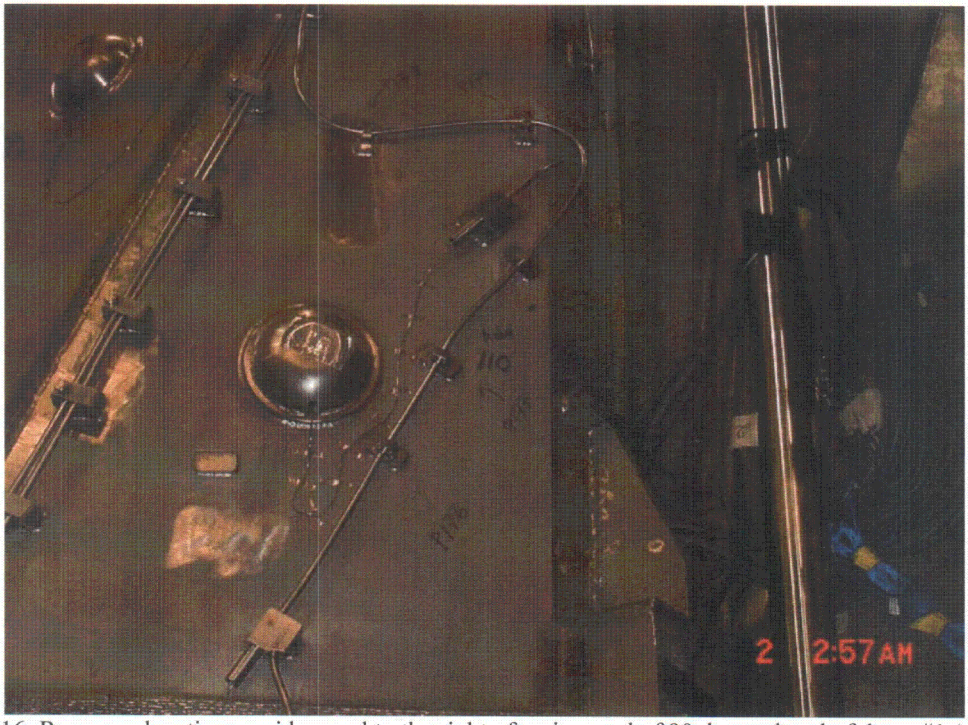

Figure 16: Response location on side panel to the right of main panel of 90 degree hood of dryer #1 (at angle w.r.t. main panel).

Figure 17: Response locations on side panel to the left of main panel of 90 degree hood of dryer #1 (at angle w.r.t. main panel).

Figure 18: Full view of 270 degree hood of dryer #1 (before installation of temporary sensors).

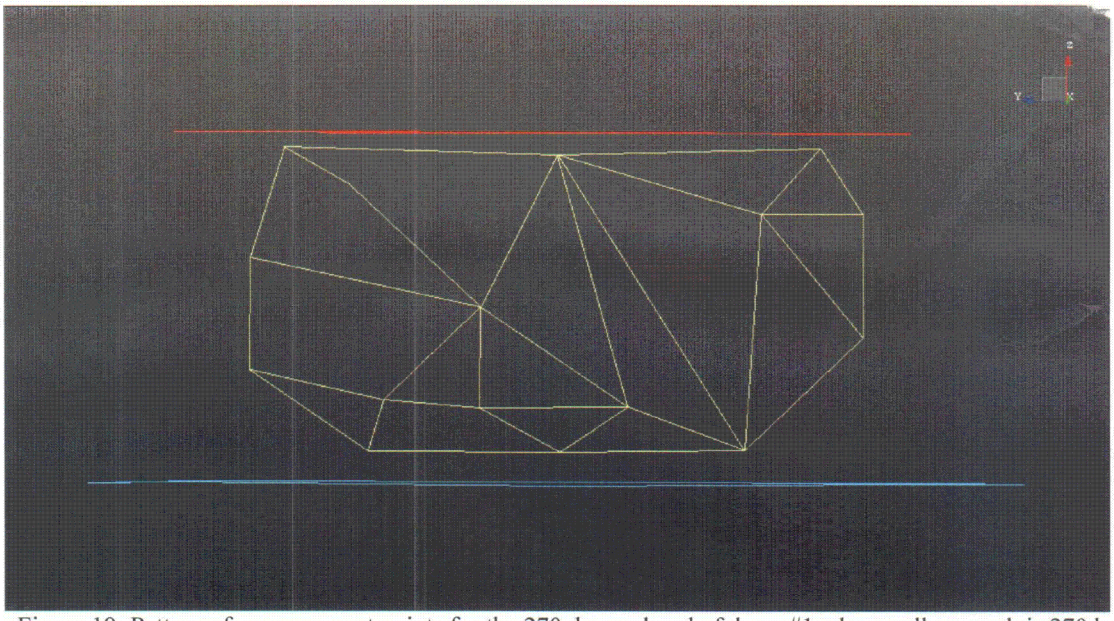

Figure 19: Pattern of measurement points for the 270 degree hood of dryer #1 where yellow mesh is 270 hood response locations, dark red is responses on top & aqua is responses on the ring.

Figure 20: Response locations on upper part of 270 degree hood of dryer #1.

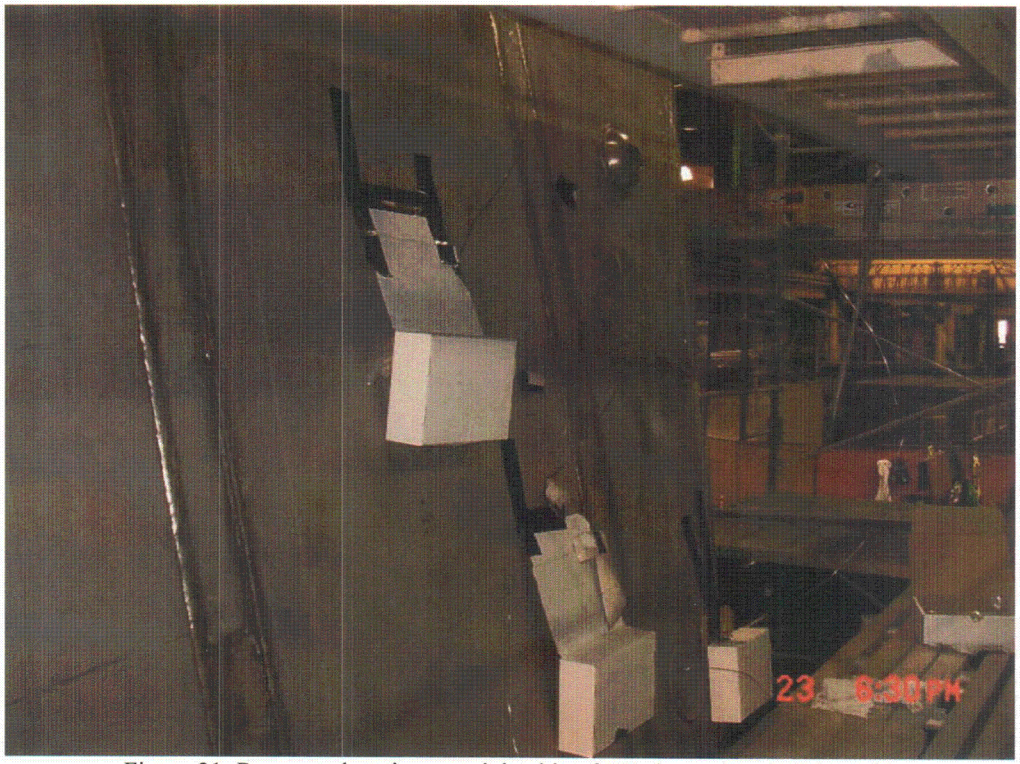

Figure 21: Response locations on right side of 270 degree hood of dryer #1

Figure 22: Response locations on lower part of 270 degree hood of dryer #1

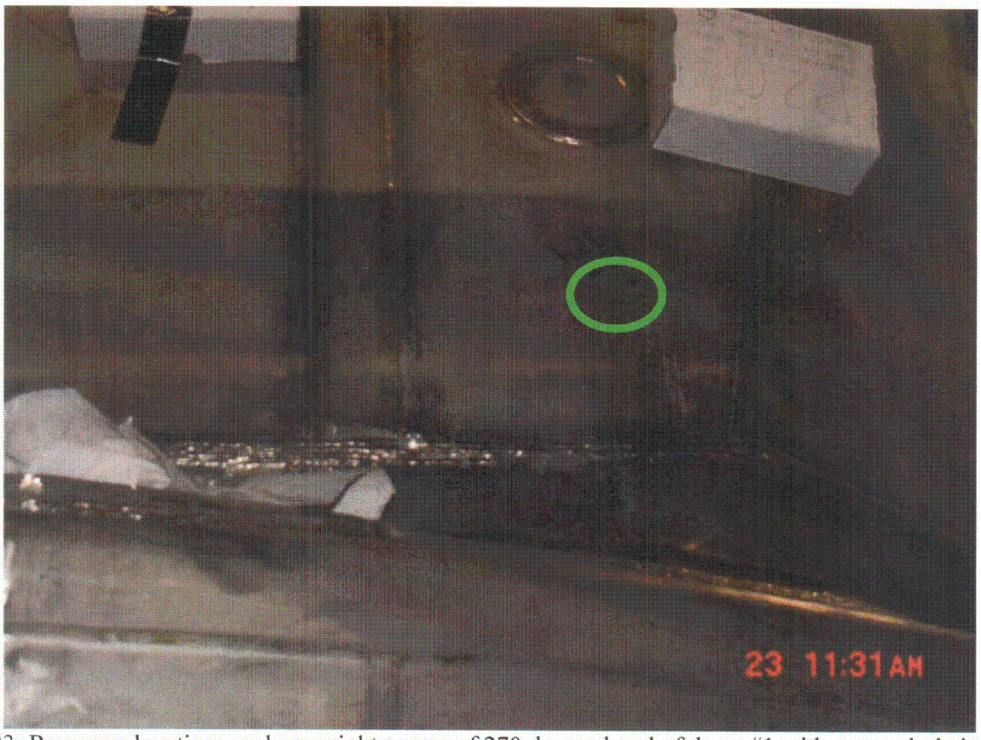

Figure 23: Response locations on lower right corner of 270 degree hood of dryer #1 with green circle indicating input location on 270 degree hood.

Figure 24: Response locations on side panel to the left of main panel of 270 degree hood of dryer #1 (at angle w.r.t. main panel).

Figure 25: Response locations on side panel to the right of main panel of 270 degree hood of dryer #1 (at angle w.r.t. main panel).

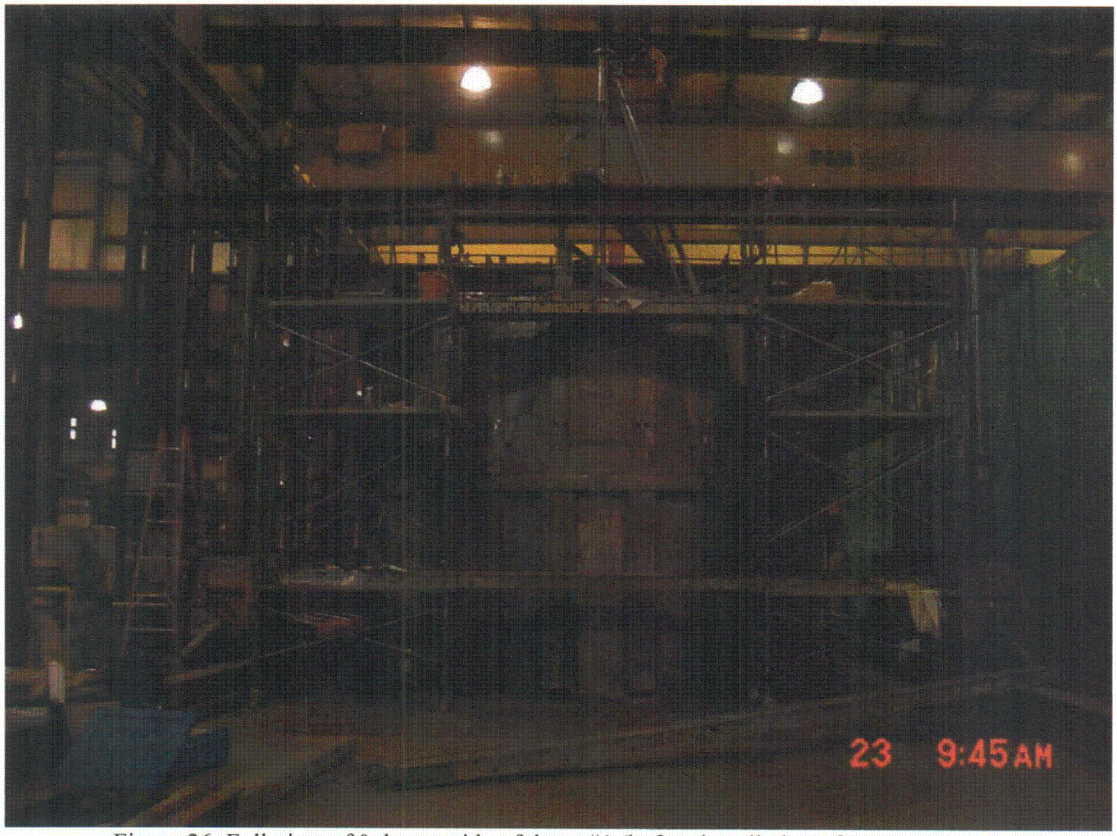

Figure 26: Full view of 0 degree side of dryer #1 (before installation of temporary sensors).

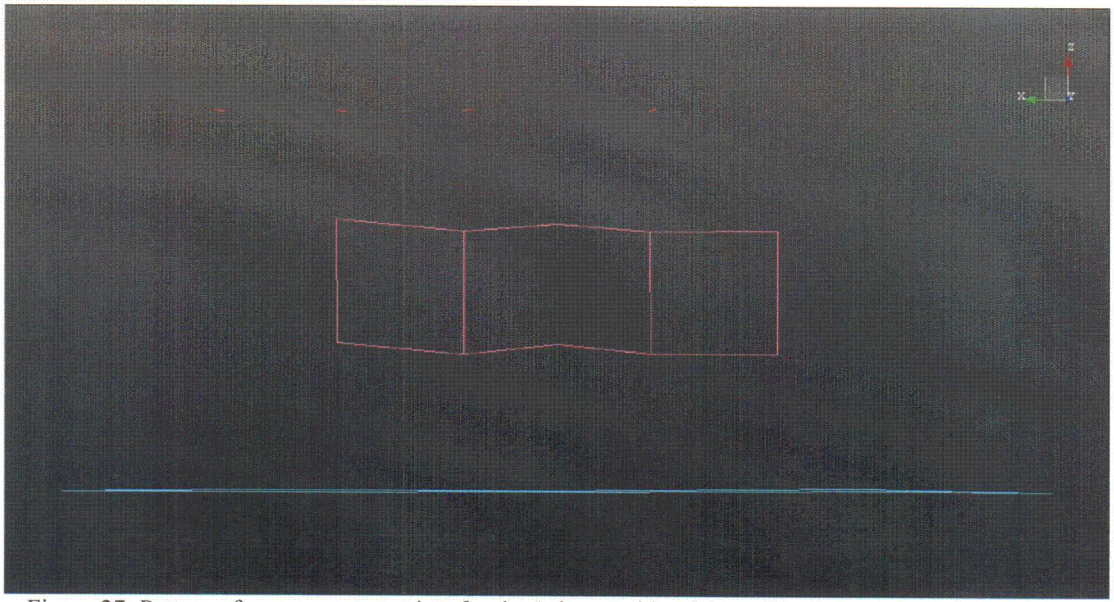

Figure 27: Pattern of measurement points for the 0 degree side of dryer #1 where pink mesh is 0 degree side response locations, dark red is responses on top & aqua is responses on the ring.

Figure 28: Response locations on left side of 0 degree side of dryer #1 with green circle indicating input location on 0 degree side

Figure 29: Response locations on middle part of 0 degree side of dryer #1.

Figure 30: Response locations on lower right part of 0 degree side of dryer #1.

Figure 31: Response locations on upper right part of 0 degree side of dryer #1.

Figure 32: Response locations on 0 degree side of dryer #1.

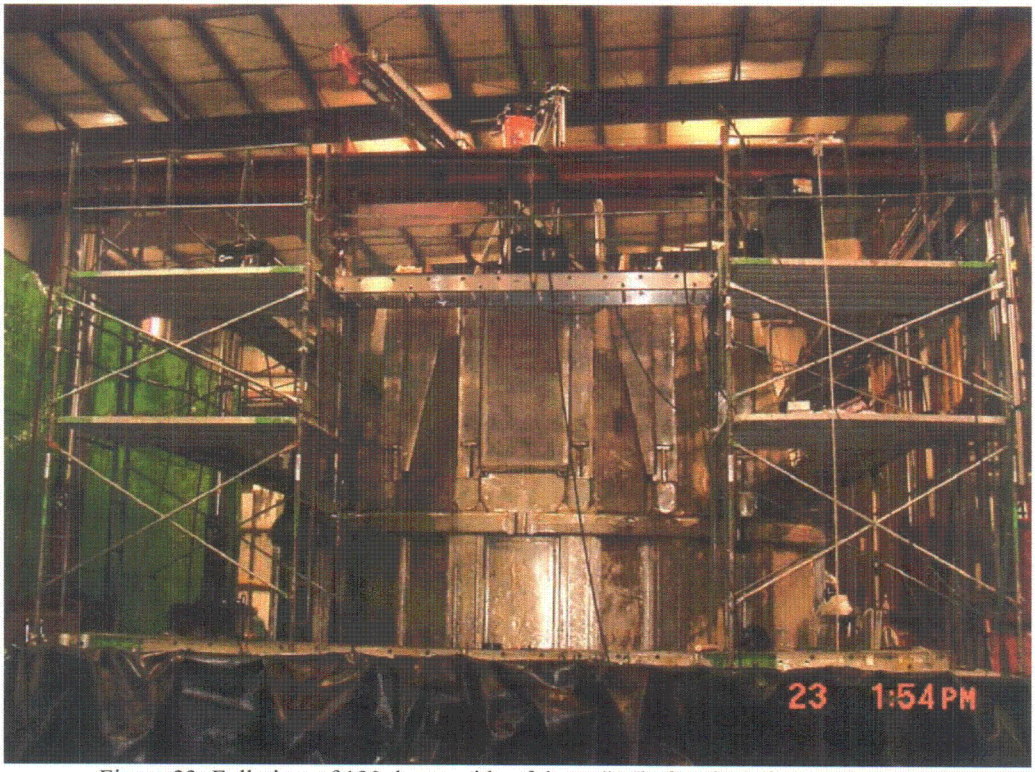

Figure 33: Full view of 180 degree side of dryer #1 (before installation of temporary sensors).

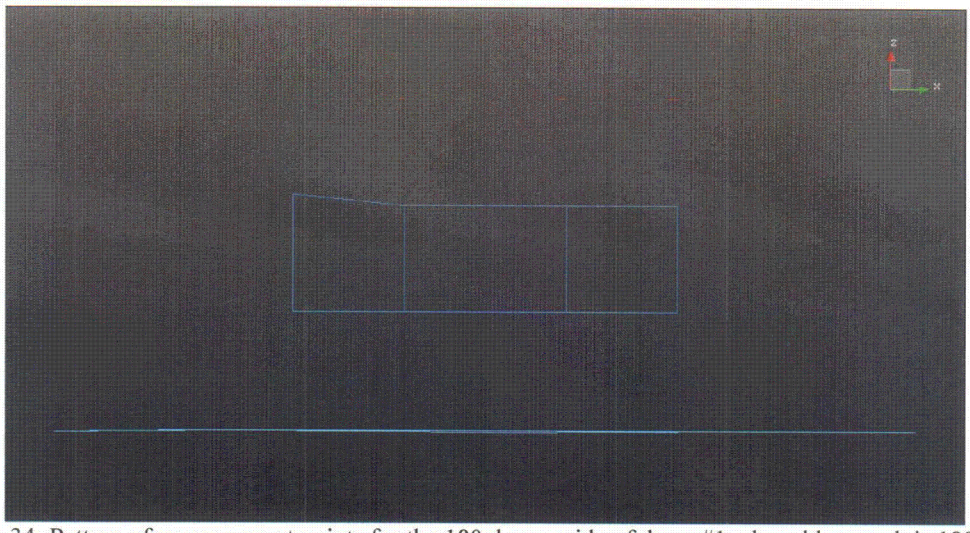

Figure 34: Pattern of measurement points for the 180 degree side of dryer #1 where blue mesh is 180 hood response locations, dark red is responses on top & aqua is responses on the ring.

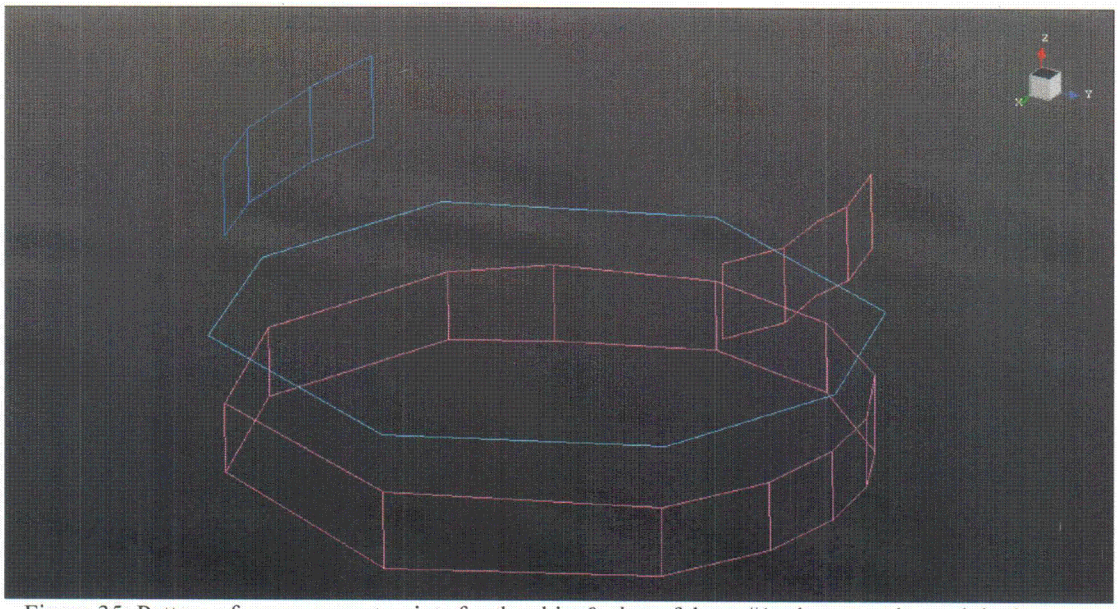

Figure 35: Pattern of measurement points for the skirt & ring of dryer #1 where purple mesh is ring response locations, aqua mesh is the response locations on the ring, blue is responses on 180 degree side & pink is responses on 0 degree side.

C01

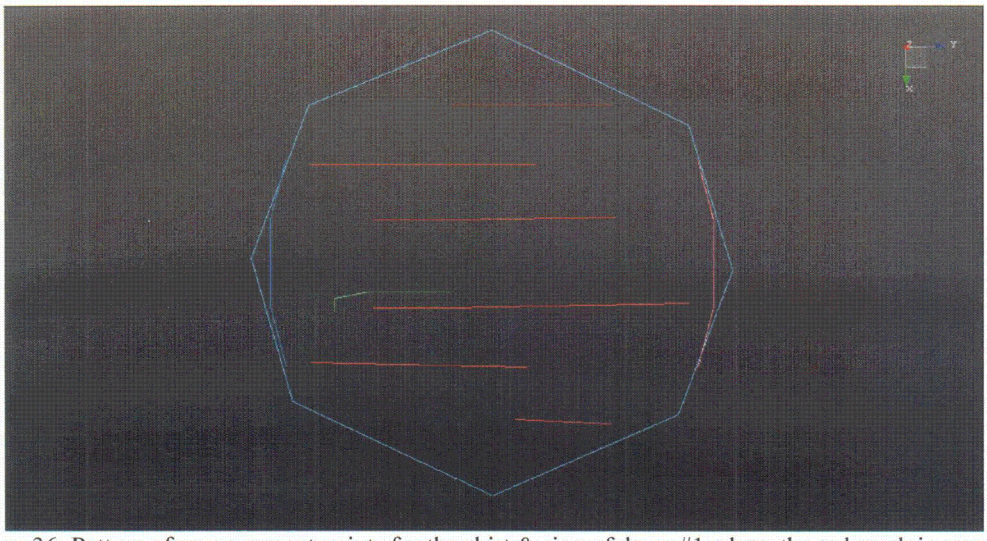

Figure 36: Pattern of measurement points for the skirt & ring of dryer #1 where the red mesh is response locations on top, green is the response locations on the panels inside the dryer, aqua is responses on the ring, blue is responses on 180 degree side & pink is responses on 0 degree side.

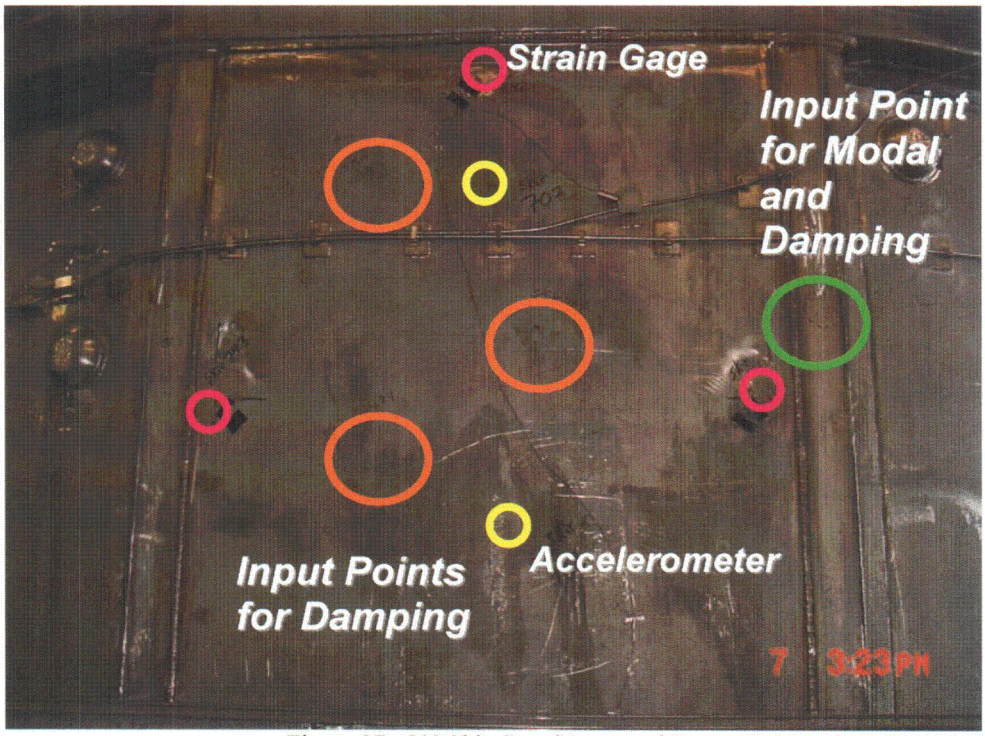

Figure 37: 90° Skirt Panel Input and Response Locations

C02

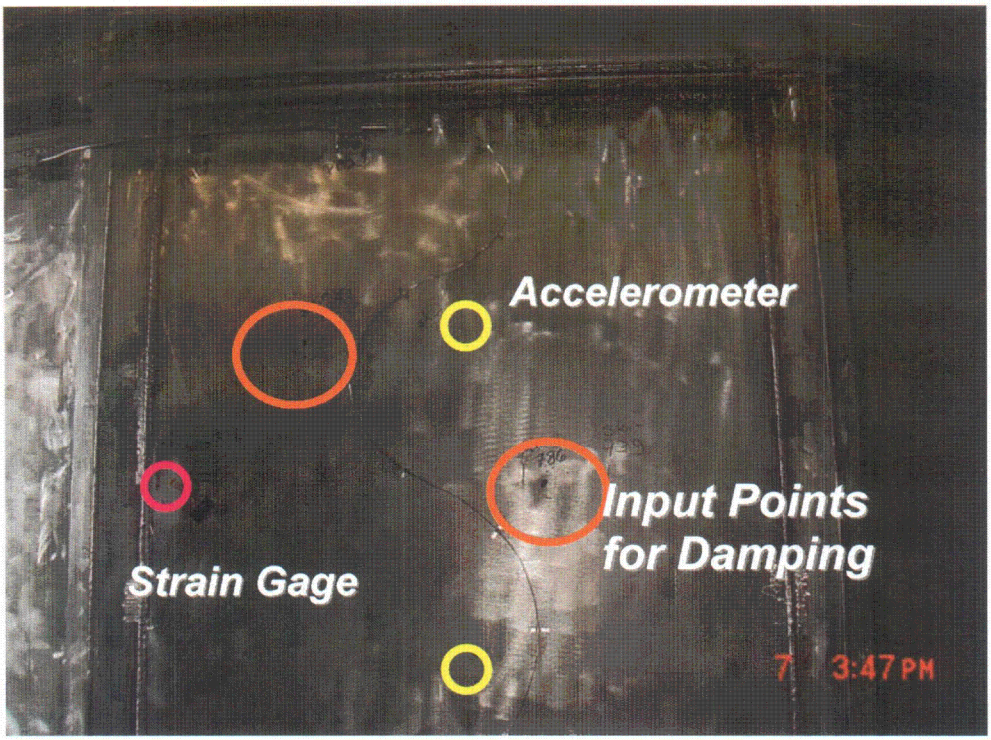

Figure 38: 270° Skirt Panel Input and Response Locations

[[

]]

Figure 39: Summation FRF for Top: Red – Test

C03

[[

]]

Figure 40: Summation FRF for 0° Side: Red – Test

[[

]]

Figure 41: Summation FRF for Skirt: Red – FE, Green - Test

[[

]]

Figure 42: FRF on 90° Skirt Panel, Upper Point: Red – FE, Green – Test, Blue – Damping Test (different input point from Green)

[[

]]

Figure 43: FRF on 90° Skirt Panel, Lower Point: Red – FE, Green – Test, Blue – Damping Test (different input point from Green)

[[

]]

Figure 44: Additional FRFs on 90° Skirt Panel, Test Measurements: Red – Left of 707 as seen in Figure 31, Green – Right of Centerline, between 707 and 708 Vertically, Blue – Upper Middle, Pink – Lower Middle

[[

]]

Figure 45: FRF on 270° Skirt Panel, Upper Point: Red – FE, Green – Test

]]

Figure 46: FRF on 270° Skirt Panel, Lower Point: Red – FE, Green – Test

[[

]]

Figure 47: FRF on 270° Skirt Panel, from Damping Test: Red – Upper Point, Green – Lower Point

[[

]]

Figure 48: FRFs on 90° and 270° Skirt Panel from Damping Test: Red -Test - 270° skirt, upper point, Green - Test - 270° skirt, lower point, Blue -Test – 90° skirt, upper point, Pink -Test - 90° skirt, lower point

[[

]]

Figure 49: Mode Shapes for Skirt, Global View: Left – Test, [[ ]]

[[

]]

Figure 50: Mode Shapes for Skirt, Local View: Left – Test, [[ ]]

[[

]]

Figure 51: Mode Shapes for Skirt, Local View: Left – Test, [[ ]]

[[

]]

Figure 52: Mode Shapes for Skirt, Local View: Left – Test, [[ ]]

[[

]]

Figure 53: Summation FRF for 90°Hood: Red – FE, Green - Test

[[

]]

Figure 54: Summation FRF for 90°Hood, FE in X-direction, Test normal to surface: Red – FE, Green - Test

[[

]]

Figure 55: MAC Matrix for 90° Hood, [[ ]]

[[

]]

Figure 56: Mode Shapes for 90° Hood, Global View: Left – Test, [[ ]]

[[

]]

Figure 57: Mode Shapes for 90° Hood, Global View: Left – Test, [[ ]]

[[

]]

Figure 58: MAC Matrix for 90° Hood, [[ ]]

[[

]]

Figure 59: Summation FRF for 270° Hood: Red – FE, Green – Test

[[

]]

Figure 60: Summation FRF for 270° Hood, FE - X-direction, Test – normal to surface (12.5° Difference): Red – FE, Green – Test

[[

]]

Figure 61: Individual FRFs for 270° Hood, FE – Top, X-direction; Middle, Y-direction; Bottom, Z-direction: Red – FE, Green – Test

[[

]]

Figure 62: Individual FRF for 270° Hood, X-direction: Red – FE, Green – Test

[[

]]

Figure 63: Mode Shapes for 270° Hood, Local View: Top – Test, [[ ]]

[[

]]

Figure 64: Mode Shapes for 270° Hood, Global View: Top – Test, [[ ]]

[[

]]

Figure 65: MAC Matrix for 270° Hood, [[ ]]

[[

]]

Figure 66: Mode Shapes for 270° Hood, Local View: Top – Test, [[ ]]

[[

]]

Figure 67: Mode Shapes for 270° Hood, Global View: Top – Test, [[ ]]

Attachment A: Steam Dryer Experimental Modal Analysis Test Plan

General Electric Steam Dryer Experimental Modal and Static Load Test

1. Equipment setup (PC, front end and cables not on dryer itself)

- 2 people
- can be done while other work is done on dryer

2. Equipment Setup (cables on dryer)

- 1 person (simultaneous with Task 3)
- can be done while other work is done on dryer as long as other work is not interfered with by cable routing

3. Geometry - node selection and preparation

- 1 person then 2 people after Task 2 is finished)
- Marking of measurement locations for accelerometers and strain gages
- Cleaning of accelerometer and strain gage locations
- can be done while some other work is done on dryer (work that is not interfered with by cable routing or accelerometer position)
- Accelerometer locations determined by PreTest and information/requests from Structural Analysis Group
- GE supposed to supply markers or paint pens allowed to be used on dryer

4. Attachment of initial accelerometer set and of strain gages

- 1 person or 2 people focus on accelerometers
- 1 person focuses on strain gages (if strain gage attachment and wiring is not finished during this specific task it will continue while accelerometers are moved later)
- can be done while some other work is done on dryer (work that is not interfered with by cable routing or accelerometer position)
- End-to-end measurement chain checks
- Initial set of locations will focus on one outer hood but include locations spread out over dryer so that quality of excitation locations can be verified
- Adhesive to be used is M-Bond 200 (a super glue with an accelerator) as it has been approved for use on the dryer
- Solvent will be acetone as it is approved for use on the dryer
- Sandpaper is Silicon Carbide paper in strain gage kit

5. Frequency Response Function (FRF) Measurements/Hammer Impact Testing

- Perform driving point measurements at support locations
- Re-verify that all transducers are operational
- Verify acceptability of excitation locations (4 to 8 excitation locations, starting with 11)
- Perform initial set of measurements dry (Current plan is to have 35 to 38 triaxial accelerometers, 1 impact hammer, and 1 single-axis driving point accelerometer in each set.
- Perform all sets of measurements wet at high water levels
- Current plan is for the first 2 sets to be spread out over dryer and the 3rd set to focus on skirt. Also, first set contains single axis accelerometers for driving point reciprocity checks.
- Perform the skirt focus set and a set with selected points from the other 2 sets at medium and low water levels

- The following pictures show the proposed excitation locations as green circles or ovals and the response locations as yellow dots.

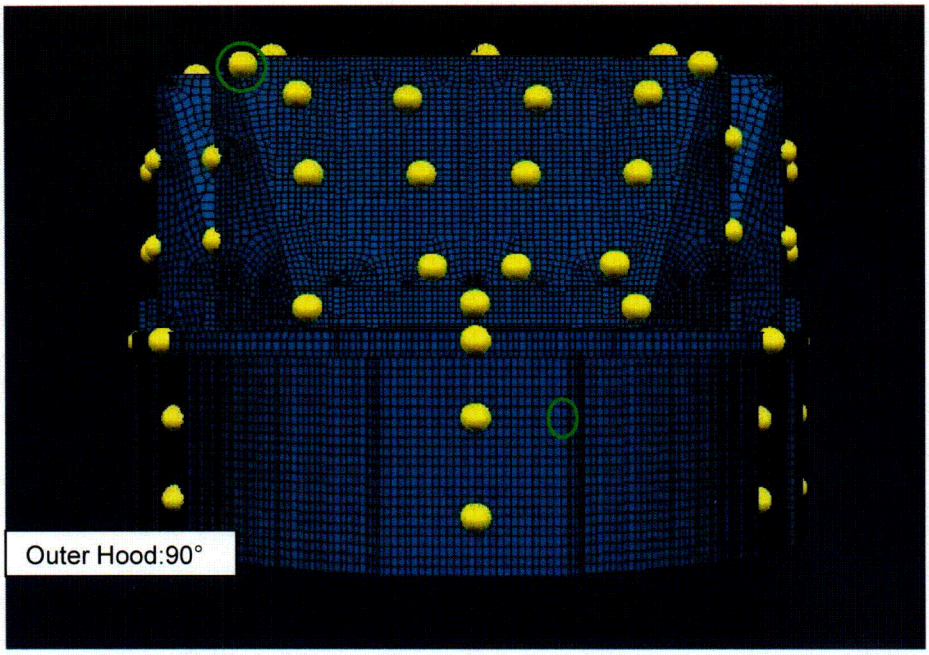

Figure A-1: 90° Side Response and Input Locations

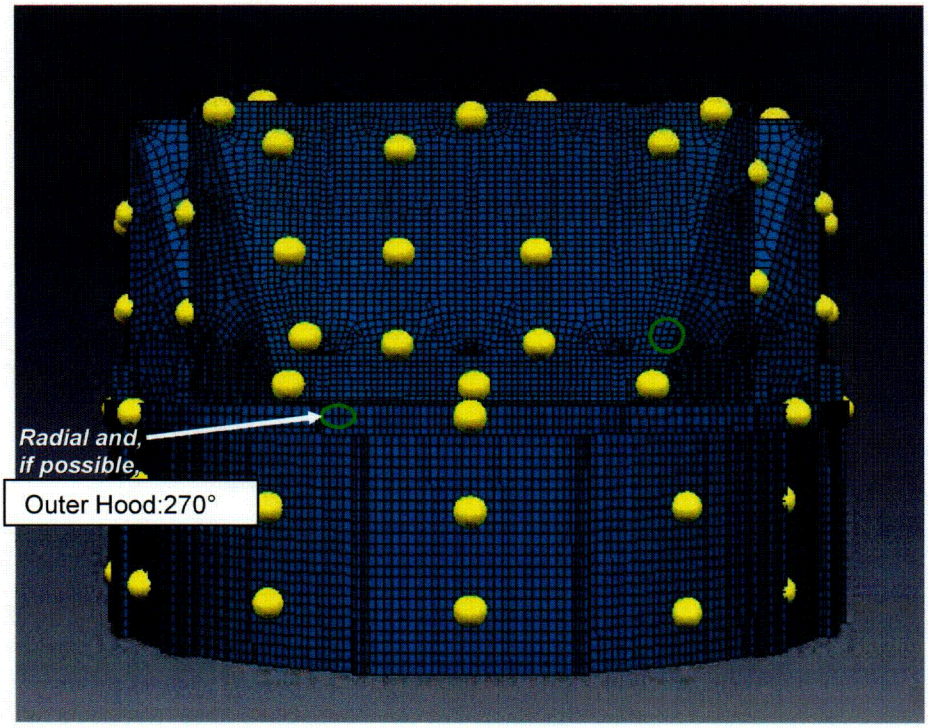

Figure A-2: 270° Side Response and Input Locations

C04

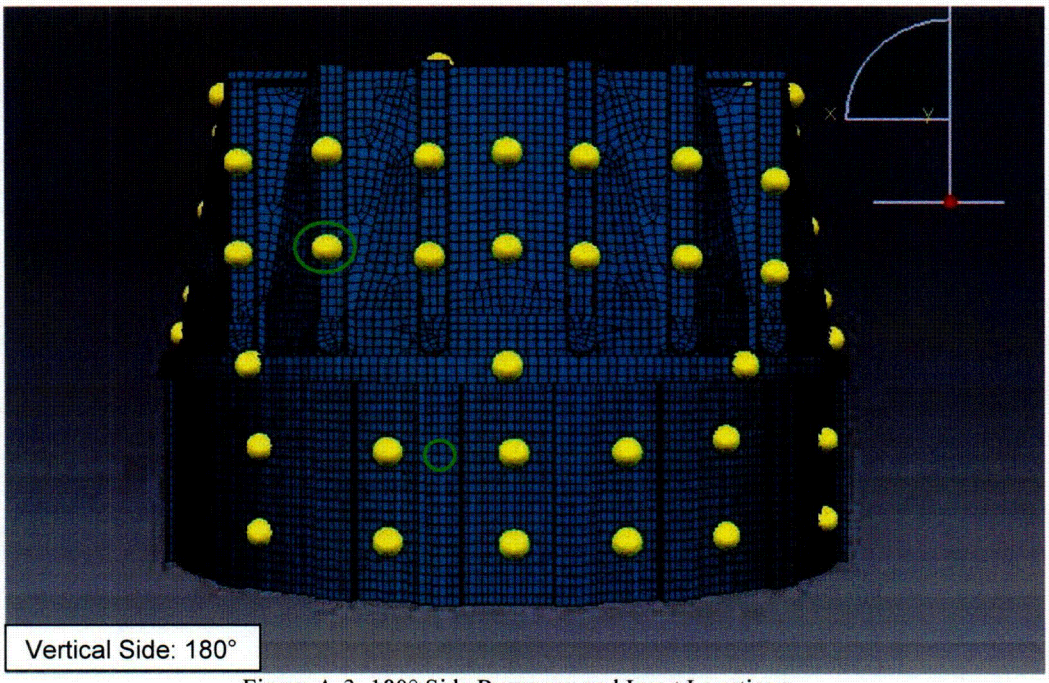

Figure A-3: 180° Side Response and Input Locations

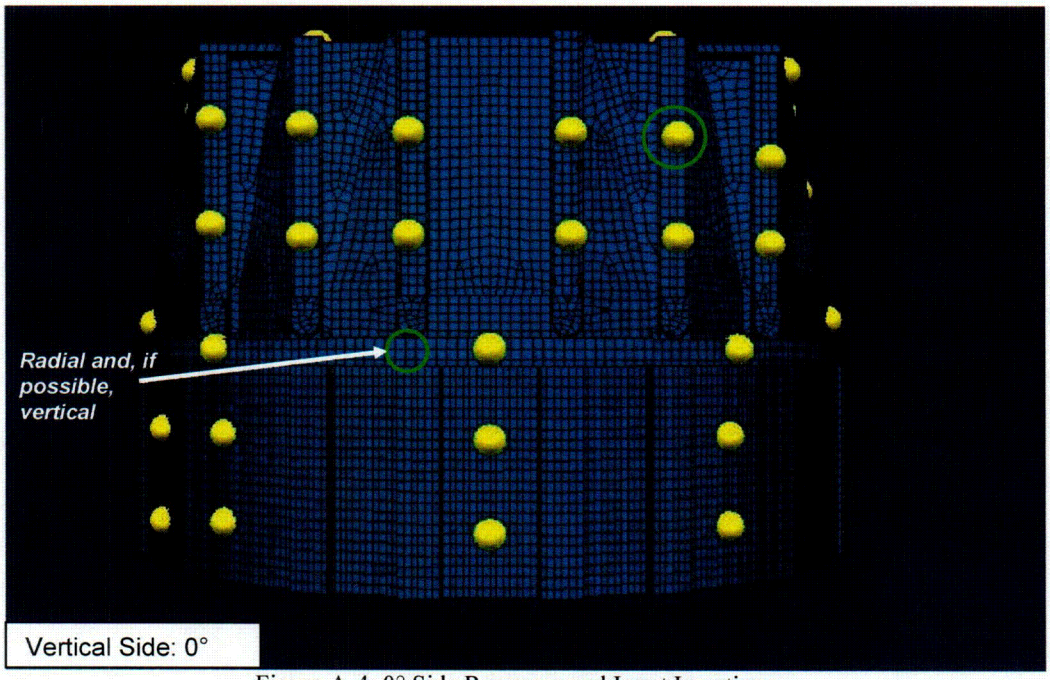

Figure A-4: 0° Side Response and Input Locations

C05

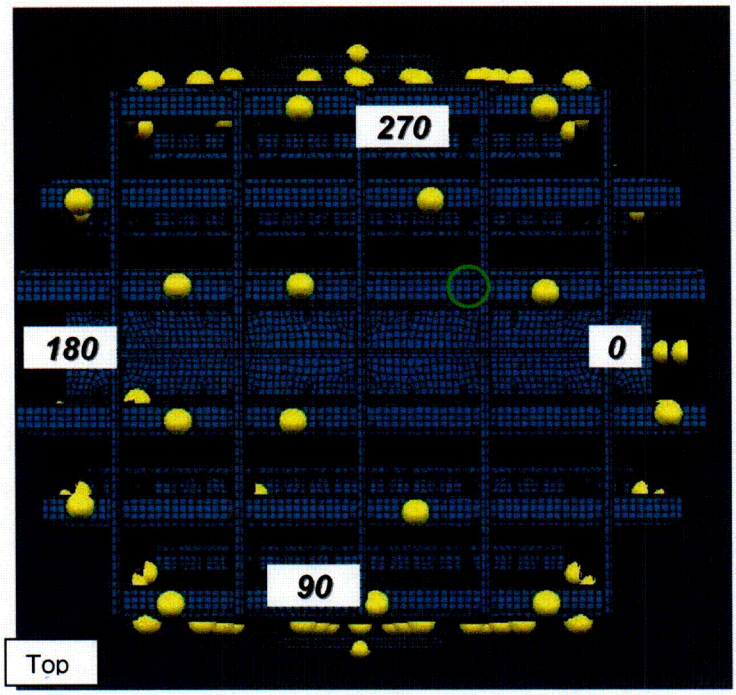

Figure A-5: Top Side Response and Input Locations

- Proposed plan for sets is included as Attachment A
- Wireframe model with node identification is included as Attachment B

Data checks include but are not limited to:

a. Review of input time records for input force and acceleration response during data acquisition
b. Review of Input Autopower
c. Review of FRF and coherence for each location (specific review of driving point)
d. Reciprocity between driving point locations
e. Repeatability of driving point measurements among sets
f. After checks for each set are done, frequency content will be available for that set
g. As sets are performed, preliminary curve-fitting will be performed to check data
h. Specific order and composition of sets still being finalized with input from structural analysis

6. Static load testing: 2 people, no other work done on dryer

a. 2 people
b. Apply 500 lb. load with hydraulic jack (assistance from JT Cullen or other required for providing backstop for jack), measure strain using 6 rosette strain gages
c. Tentative Load application location – Outer hood near MSL nozzle location – still being reviewed as are strain gage locations

C06

7. Final hammer impact measurements if necessary

    a. 2 or 3 people
    b. Repeat any points where data was inadequate for any reason or add additional points as determined by review during data acquisition
    c. Would be determined by analysis and processing done along way and while static load testing is performed

8. Removal of accelerometers and cables on dryer

    a. 2 or 3 people
    b. can be done while some other work is done on dryer (work that is not interfered with by cable routing or accelerometer position)
    c. Discussion will occur with GE about timing. If it makes sense, 1 person will continue processing data while 1 or 2 others remove accelerometers based on need to make dryer available.

9. Surface cleanup

    a. 2 or 3 people
    b. can be done while other work is done on dryer or while dryer is at plant (proposed in late January by GE)
    c. Discussion will occur with GE about timing. If it makes sense, 1 person will continue processing data while 1 or 2 others remove accelerometers based on need to make dryer available.

10. Equipment breakdown (PC, front end and cables not on dryer)

    a. 2 or 3 people
    b. can be done while other work is done on dryer

Attachment A of Report Att. A– Proposed Sets of Measurement Locations/Nodes

Set A	Set B	Set C
Impact Hammer	Impact Hammer	Impact Hammer
Driving Point	Driving Point	Driving Point
301	302	810
814	811	813
809	303	812
804	806	807
606	808	805
801	802	803
602/681	601	110
604	603	704
404	605	734
608	607	731
610	609	206
207	208	205
508	215	507
506	505	713
504	503	714
501/581	114	710
119	117	111
412/121	115	118
103	107	104
101	109	108
106	401	705
105	102	707
402/120	403	708
112	113	711
406/218	725	726
405	728	729
702	735	732
116/181	502	205
210	202	209
204	203	202
216	214	217
211	212	201
213	407	722
408/219	719	716
723	720	717
	410	411
	Repeats or Extra	Repeats or Extra
	Repeats or Extra	Repeats or Extra

Triaxes replaced by single axis accels at driving points for reciprocity

e07

Attachment B of Report Att. A – Wireframe with Measurement Points/Node Numbers

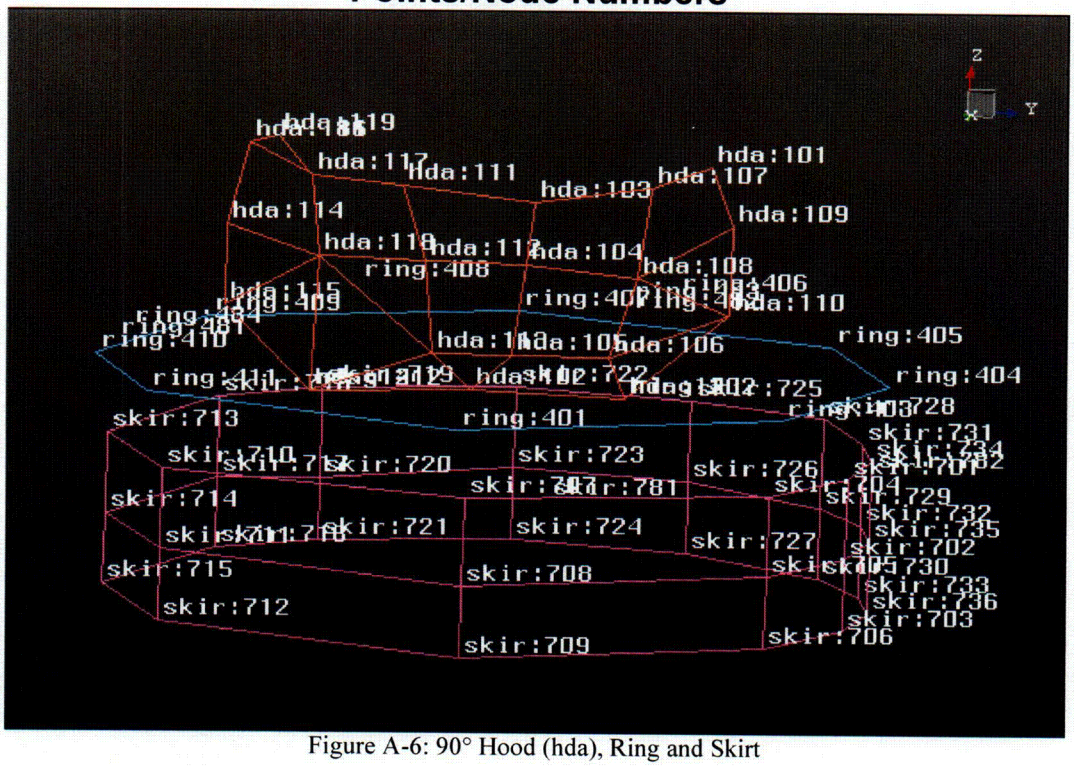

Figure A-6: 90° Hood (hda), Ring and Skirt

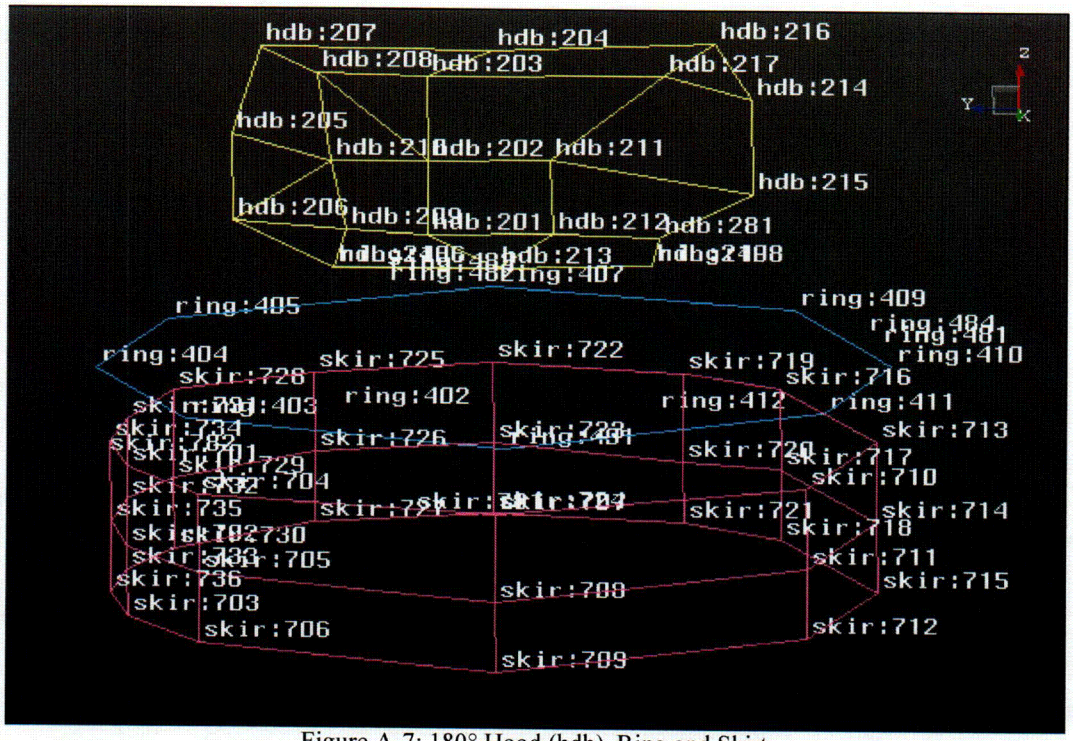

Figure A-7: 180° Hood (hdb), Ring and Skirt

C09

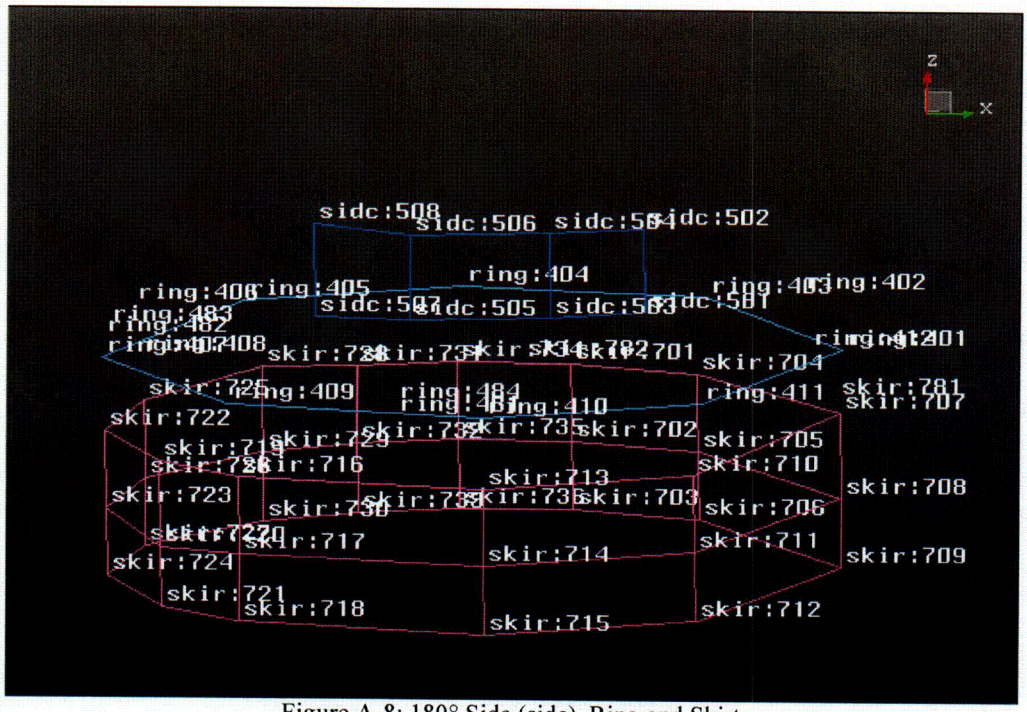

Figure A-8: 180° Side (sidc), Ring and Skirt

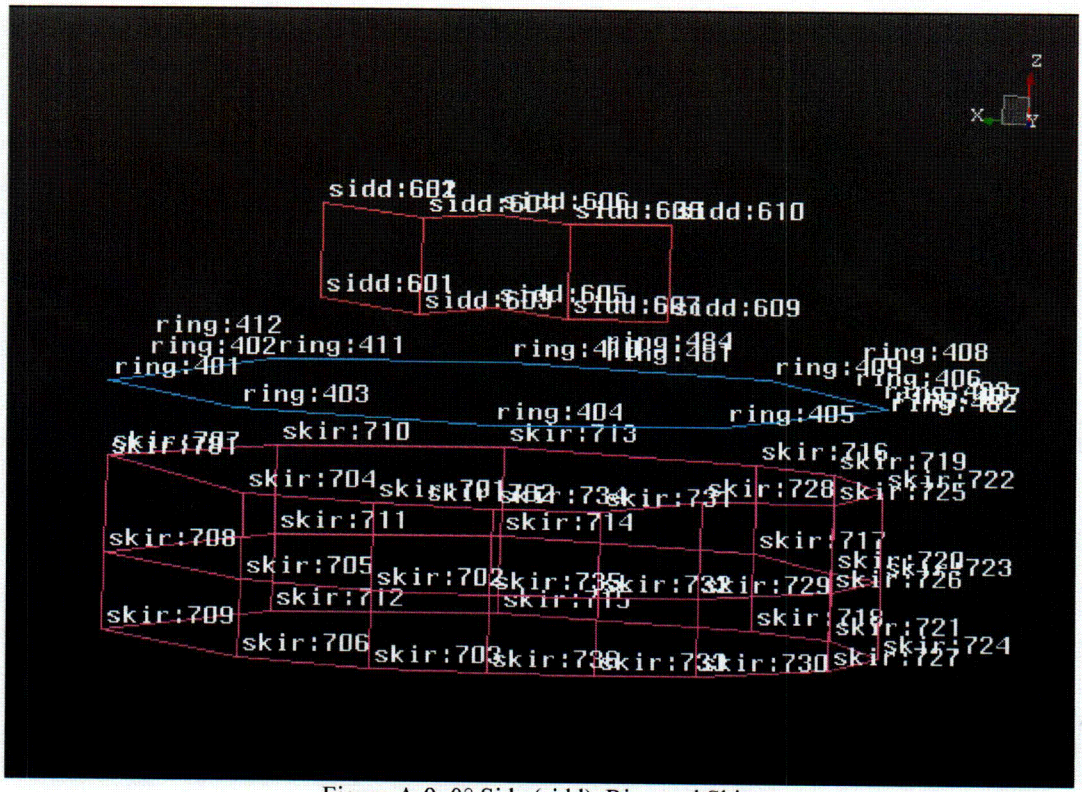

Figure A-9: 0° Side (sidd), Ring and Skirt

C09

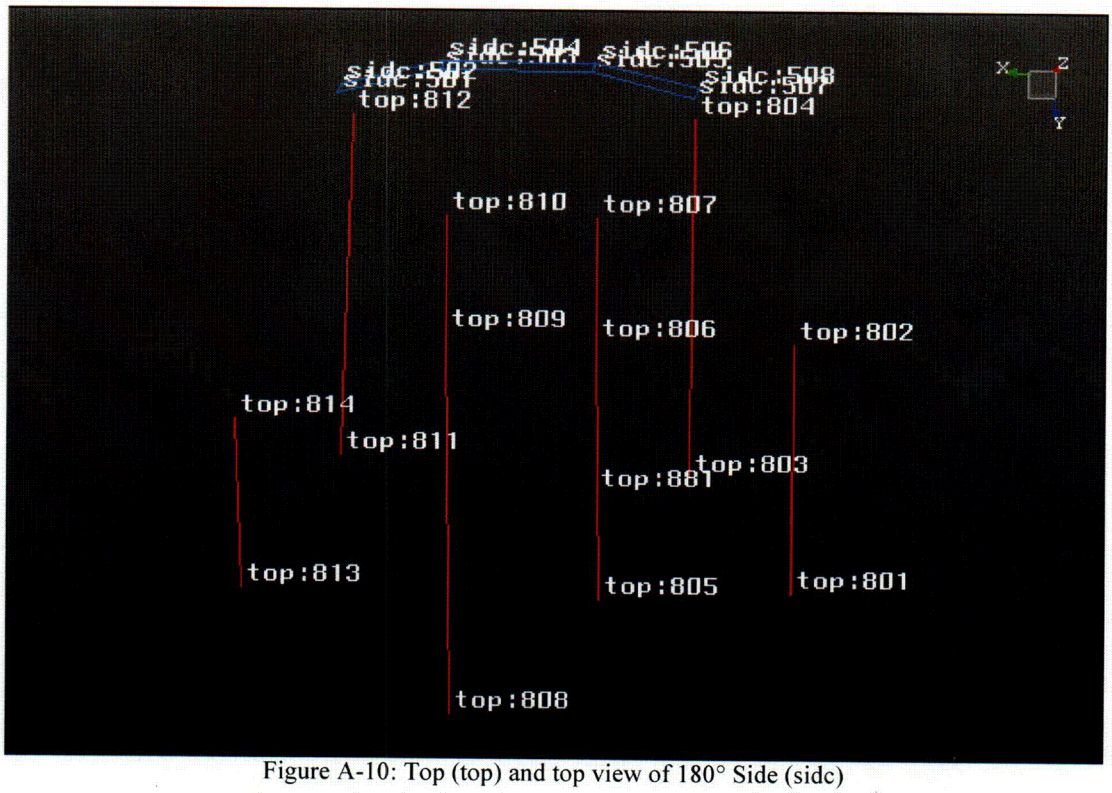

Figure A-10: Top (top) and top view of 180° Side (sidc)

C10

Attachment B: Skirt Sub-Model Study

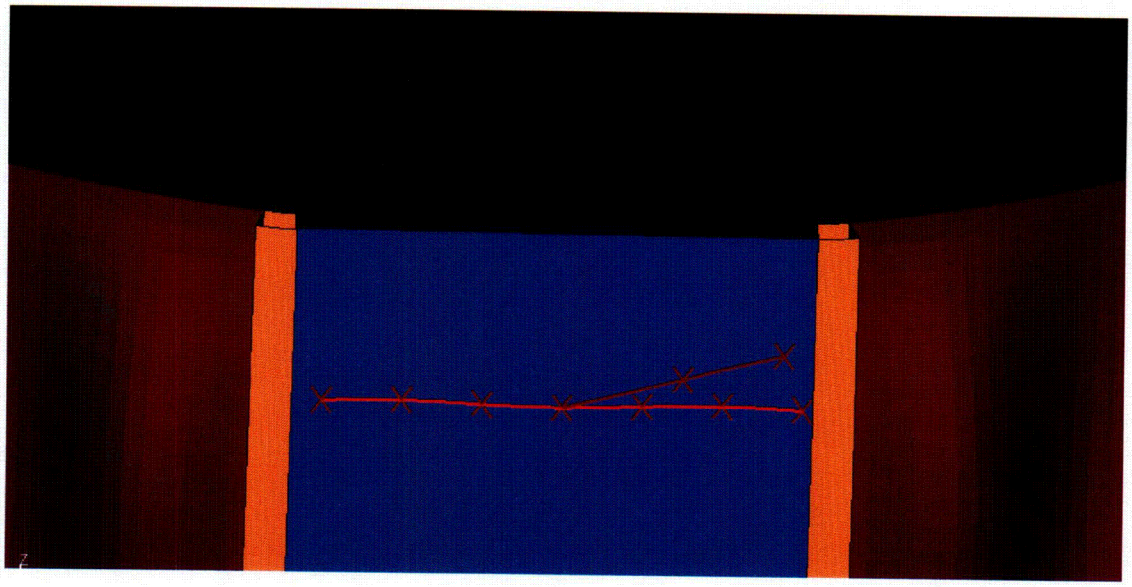

Figure B-1: Location of Conduit and Instrumentation Pads on Skirt Panel

[[

Figure B-2 Left – Baseline, [[ ]]]]

C11

[[

]]

Figure B-3: Left – Baseline, [[ ]]

[[

]]

Figure B-4: Left – Baseline, [[ ]]

[[

]]

Figure B-5: Left – Baseline, [[ ]]

]]

Figure B-6: Left – Baseline, [[ ]]

[[

]]

Figure B-7: Left – Baseline, [[ ]]

Attachment C: Effect of Number of Averages

This attachment illustrates how the FRF measurement and coherence are affected when a different number of hammer impacts is used. Two measurements have been taken with the same excitation and response locations, one measurement with twenty hammer impacts and one measurement with five hammer impacts. The data presented in the following figures was measured on the 90 degree and 270 degree skirt panels of Dryer #2 (the dryer without permanent sensors intended for Quad Cities Unit # 1 (QC1)).

Specific measurements show some difference between 20 averages and 5 averages, particularly near [[ ]]. Theses differences are attributed to inconsistency in the hammer impact. In general, the frequency, shape, and phase of the FRF are consistent between 20 averages and 5 averages. The phase of the FRF is generally "cleaner" with 20 averages as well. The coherence shows some differences between 20 averages and 5 averages, but the differences appear to be specific to individual measurements and usually at low frequency – below [[ ]]. The other coherence differences are near [[ ]] and correspond to those measurements with some difference in FRF amplitude that has been attributed to inconsistency in the hammer impact.

[[

]]

Figure E-1: Comparison of the FRF amplitude, FRF phase and coherence between a hammer impact measurement with 20 averages (red) and one with 5 averages (green) for normal excitation at point skir:785 and normal response at point skir:785 on the 90 degree skirt panel of Dryer #2

[[

]]

Figure E-2: Comparison of the FRF amplitude, FRF phase and coherence between a hammer impact measurement with 20 averages (red) and one with 5 averages (green) for normal excitation at point skir:785 and normal response at point skir:753 on the 90 degree skirt panel of Dryer #2

[[

]]

Figure E-3: Comparison of the FRF amplitude, FRF phase and coherence between a hammer impact measurement with 20 averages (red) and one with 5 averages (green) for normal excitation at point skir:785 and normal response at point skir:707 on the 90 degree skirt panel of Dryer #2

[[

]]

Figure E-4: Comparison of the FRF amplitude, FRF phase and coherence between a hammer impact measurement with 20 averages (red) and one with 5 averages (green) for normal excitation at point skir:785 and normal response at point skir:722 on the 270 degree skirt panel of Dryer #2

[[

]]

Figure E-5: Comparison of the FRF amplitude, FRF phase and coherence between a hammer impact measurement with 20 averages (red) and one with 5 averages (green) for normal excitation at point skir:785 and normal response at point skir:762 on the 270 degree skirt panel of dryer 2

[[

]]

Figure E-6: Comparison of the FRF amplitude, FRF phase and coherence between a hammer impact measurement with 20 averages (red) and one with 5 averages (green) for normal excitation at point skir:785 and response at strain gage channel C at point skir:796 on the 90 degree skirt panel of Dryer #2

Attachment D: Acquisition Front-end channel assignment

A/D CHANNEL ASSIGNMENT DRY SET A

A/D CHASSIS: 2 LMS Scadas III frontends in master-slave setup

A/D CHANNEL	SENSOR ID	A/D CHANNEL	SENSOR ID	A/D CHANNEL	SENSOR ID	A/D CHANNEL	SENSOR ID
1	21233	33	37277_X	65	16224_Z	97	16684_Y
2		34	37277_Y	66	15625_X	98	16684_Z
3	36614_X	35	37277_Z	67	15625_Y	99	16955_X
4	36614_Y	36	37278_X	68	15625_Z	100	16955_Y
5	36614_Z	37	37278_Y	69	17051_X	101	16955_Z
6	36616_X	38	37278_Z	70	17051_Y	102	20267_X
7	36616_Y	39	37279_X	71	17051_Z	103	20267_Y
8	36616_Z	40	37279_Y	72	17333_X	104	20267_Z
9	21836	41	37279_Z	73	17333_Y	105	220_X
10	21860	42	37280_X	74	17333_Z	106	264_Y
11	21852	43	37280_Y	75	27796_X	107	8751_Z
12	21855	44	37280_Z	76	27796_Y	108	8754_X
13	21857	45	37281_X	77	27796_Z	109	8777_Y
14	NA	46	37281_Y	78	27800_X	110	8778_Z
15	37126_X	47	37281_Z	79	27800_Y	111	8766_X
16	37126_Y	48	21869	80	27800_Z	112	8767_Y
17	37126_Z	49	22143	81	31423_X	113	8768_Z
18	37129_X	50		82	31423_Y	114	11156_X
19	37129_Y	51	37283_X	83	31423_Z	115	18026_Y
20	37129_Z	52	37283_Y	84	31425_X	116	19586_Z
21	37130_X	53	37283_Z	85	31425_Y		
22	37130_Y	54	15514_X	86	31425_Z		
23	37130_Z	55	15514_Y	87	31426_X		
24	37131_X	56	15514_Z	88	31426_Y		
25	37131_Y	57	15990_X	89	31426_Z		
26	37131_Z	58	15990_Y	90	15314_X		
27	37132_X	59	15990_Z	91	15314_Y		
28	37132_Y	60	15591_X	92	15314_Z		
29	37132_Z	61	15591_Y	93	15333_X		
30	37275_X	62	15591_Z	94	15333_Y		
31	37275_Y	63	16224_X	95	15333_Z		
32	37275_Z	64	16224_Y	96	16684_X		

Data Collected By: **Signature:**

Verified By: **Signature:**

Date Performed:

Test Equip., Serial No. & Calibration Due Date:

LMS Scadas III frontend (master)	41011904	09-Mar-06
LMS Scadas III frontend (slave)	41001503	15-Feb-06

A/D CHANNEL ASSIGNMENT DRY SET B LWL SET A HWL SET A LWL SET C

A/D CHASSIS: 2 LMS Scadas III frontends in master-slave setup

A/D CHANNEL	SENSOR ID	A/D CHANNEL	SENSOR ID	A/D CHANNEL	SENSOR ID	A/D CHANNEL	SENSOR ID
1	21233	33	37277_X	65	16224_Z	97	16684_Y
2	37322	34	37277_Y	66	15625_X	98	16684_Z
3	36614_X	35	37277_Z	67	15625_Y	99	16955_X
4	36614_Y	36	37278_X	68	15625_Z	100	16955_Y
5	36614_Z	37	37278_Y	69	17051_X	101	16955_Z
6	36616_X	38	37278_Z	70	17051_Y	102	20267_X
7	36616_Y	39	37279_X	71	17051_Z	103	20267_Y
8	36616_Z	40	37279_Y	72	17333_X	104	20267_Z
9	37124_X	41	37279_Z	73	17333_Y	105	220_X
10	37124_Y	42	37280_X	74	17333_Z	106	264_Y
11	37124_Z	43	37280_Y	75	27796_X	107	8751_Z
12	37125_X	44	37280_Z	76	27796_Y	108	8754_X
13	37125_Y	45	37281_X	77	27796_Z	109	8777_Y
14	37125_Z	46	37281_Y	78	27800_X	110	8778_Z
15	37126_X	47	37281_Z	79	27800_Y	111	8766_X
16	37126_Y	48	37282_X	80	27800_Z	112	8767_Y
17	37126_Z	49	37282_Y	81	31423_X	113	8768_Z
18	37129_X	50	37282_Z	82	31423_Y	114	11156_X
19	37129_Y	51	37283_X	83	31423_Z	115	18026_Y
20	37129_Z	52	37283_Y	84	31425_X	116	19586_Z
21	37130_X	53	37283_Z	85	31425_Y		
22	37130_Y	54	15514_X	86	31425_Z		
23	37130_Z	55	15514_Y	87	31426_X		
24	37131_X	56	15514_Z	88	31426_Y		
25	37131_Y	57	15990_X	89	31426_Z		
26	37131_Z	58	15990_Y	90	15314_X		
27	37132_X	59	15990_Z	91	15314_Y		
28	37132_Y	60	15591_X	92	15314_Z		
29	37132_Z	61	15591_Y	93	15333_X		
30	37275_X	62	15591_Z	94	15333_Y		
31	37275_Y	63	16224_X	95	15333_Z		
32	37275_Z	64	16224_Y	96	16684_X		

Data Collected By: **Signature:**

Verified By: **Signature:**

Date Performed:

Test Equip., Serial No. & Calibration Due Date:

LMS Scadas III frontend (master)	41011904	09-Mar-06
LMS Scadas III frontend (slave)	41001503	15-Feb-06

A/D CHANNEL ASSIGNMENT

DRY SET C DRY SET D LWL SET D MWL SET D
HWL SET D HWL SET B MWL SET B LWL SET B

A/D CHASSIS: 2 LMS Scadas III frontends in master-slave setup

A/D CHANNEL	SENSOR ID	A/D CHANNEL	SENSOR ID	A/D CHANNEL	SENSOR ID	A/D CHANNEL	SENSOR ID
1	21233	33	37277_X	65	16224_Z	97	16684_Y
2	37322	34	37277_Y	66	15625_X	98	16684_Z
3	36614_X	35	37277_Z	67	15625_Y	99	16955_X
4	36614_Y	36	37278_X	68	15625_Z	100	16955_Y
5	36614_Z	37	37278_Y	69	17051_X	101	16955_Z
6	36616_X	38	37278_Z	70	17051_Y	102	20267_X
7	36616_Y	39	37279_X	71	17051_Z	103	20267_Y
8	36616_Z	40	37279_Y	72	17333_X	104	20267_Z
9	17998	41	37279_Z	73	17333_Y	105	220_X
10	18004	42	37280_X	74	17333_Z	106	264_Y
11	18011	43	37280_Y	75	27796_X	107	8751_Z
12	21870	44	37280_Z	76	27796_Y	108	8754_X
13	NA	45	37281_X	77	27796_Z	109	8777_Y
14	NA	46	37281_Y	78	27800_X	110	8778_Z
15	37126_X	47	37281_Z	79	27800_Y	111	8766_X
16	37126_Y	48	37282_X	80	27800_Z	112	8767_Y
17	37126_Z	49	37282_Y	81	31423_X	113	8768_Z
18	37129_X	50	37282_Z	82	31423_Y	114	11156_X
19	37129_Y	51	37283_X	83	31423_Z	115	18026_Y
20	37129_Z	52	37283_Y	84	31425_X	116	19586_Z
21	37130_X	53	37283_Z	85	31425_Y		
22	37130_Y	54	15514_X	86	31425_Z		
23	37130_Z	55	15514_Y	87	31426_X		
24	37131_X	56	15514_Z	88	31426_Y		
25	37131_Y	57	15990_X	89	31426_Z		
26	37131_Z	58	15990_Y	90	15314_X		
27	37132_X	59	15990_Z	91	15314_Y		
28	37132_Y	60	15591_X	92	15314_Z		
29	37132_Z	61	15591_Y	93	15333_X		
30	37275_X	62	15591_Z	94	15333_Y		
31	37275_Y	63	16224_X	95	15333_Z		
32	37275_Z	64	16224_Y	96	16684_X		

Data Collected By: _____ **Signature:** _____

Verified By: _____ **Signature:** _____

Date Performed: _____

Test Equip., Serial No. & Calibration Due Date:

LMS Scadas III frontend (master)	41011904	09-Mar-06
LMS Scadas III frontend (slave)	41001503	15-Feb-06

A/D CHANNEL ASSIGNMENT	DRY SET E	LWL SET E	MWL SET E	HWL SET E

A/D CHASSIS:	2 LMS Scadas III frontends in master-slave setup

A/D CHANNEL	SENSOR ID	A/D CHANNEL	SENSOR ID	A/D CHANNEL	SENSOR ID	A/D CHANNEL	SENSOR ID
1	Strain	33	37280_Y				
2	Strain	34	37280_Z				
3	Strain	35	NA				
4	Strain	36	NA				
5	Strain						
6	Strain						
7	Strain						
8	Strain						
9	Strain						
10	Strain						
11	Strain						
12	Strain						
13	NA						
14	NA						
15	NA						
16	NA						
17	NA						
18	NA						
19	NA						
20	NA						
21	21233						
22	37322						
23	27796_X						
24	27796_Y						
25	27796_Z						
26	37132_X						
27	37132_Y						
28	37132_Z						
29	37279_X						
30	37279_Y						
31	37279_Z						
32	37280_X						

Data Collected By: _____ **Signature:** _____

Verified By: _____ **Signature:** _____

Date Performed: _____

Test Equip., Serial No. & Calibration Due Date: _____

A/D CHANNEL ASSIGNMENT Static load test

A/D CHASSIS: 2 LMS Scadas III frontends in master-slave setup

A/D CHANNEL	SENSOR ID	A/D CHANNEL	SENSOR ID	A/D CHANNEL	SENSOR ID	A/D CHANNEL	SENSOR ID
1	Strain						
2	Strain						
3	Strain						
4	Strain						
5	Strain						
6	Strain						
7	Strain						
8	Strain						
9	NA						
10	NA						
11	NA						
12	NA						
13	NA						
14	NA						
15	NA						
16	NA						
17	NA						
18	NA						
19	NA						
20	NA						

Data Collected By: **Signature:**

Verified By: **Signature:**

Date Performed:

Test Equip., Serial No. & Calibration Due Date:

Attachment E: Test Log Sheets

(1)

Data Log — Dryer Modal

Project: ModImpact Dry050402a.lms

Section / Title of Test	Impact Hammer Location	Data Filename (Run)	Date and Time of Acquisition	Comments / Gain Settings
		DT 050402		
See Run Notes * SetA	Ring:481:+Y	Ring481+Y1	050402 0930	
		Ring481+Y2		
		Ring481+Y3		Change to a .25Hz LP
Project: Dry050402a.lms				
SetA	Ring:481:+Y	Ring481+Y1	050402 1110	Change to 0.125Hz LP
		Ring481+Y2		
		Ring481+Y3		
		Ring481+Y4		
	Ring:484:-Z	Ring484-Z1	NG - Slight double	
		Ring484-Z2	050402 1125 HRT	
		Ring484-Z3		
		Ring484-Z4	050402 1127	
Project: ModImpactDry050402a.lms				
SetA	Ring:484:-Z	Ring484-Z1	050402 1140	
		Ring484-Z2		
		Ring484-Z3		
		Ring484-Z4		red tip Lyr hit
		Ring484-Z5	050402 1254	red tip
	Top:881:-Z	Top881-Z1	050402 1330	gray tip
		Top881-Z2		
		Top881-Z3		
		Top881-Z4	1351	red tip
Project: Dry050402a.lms				
	Top:881:-Z	Top881-Z1	050402 1353	gray tip Did not Trigger at correct Time
		Top881-Z2		
		Top881-Z3		Did not Trigger at correct Time
		Top881-Z4	1400	let capture event

Data Collected By: De Brabandere/Neiheisel Signature: D. Brabandere/Neiheisel

Verified By: Melitz Signature: [signature]

Date Performed: 050402

Test Equip., Serial No. & Calibration Due Date:

(2)

Data Log — Dryer Medal

(Section) Title of Test	Impact Hammer Location	(Run) Data Filename	Date and Time of Acquisition		Comments Gain Settings
Project: ModImpact Dry 050402a. lms					
SetA	Ring:481:-Y	sidd681-Y1	050402	1445	red tip
	hda:182:-X	hda182-X1			red tip
		hda182-X2			brown tip 2 hits
		hda182-X3			black tip 3 hits
	hdb:281:+X	hdb281-X1	050402	1616	switched to gray tip
	ring:482:+X	ring482+X1			
	ring:483:-Z	ring483-Z1			
		ring483-Z2			
	skir:781:-X	skir781-X1	050402	1755	
Project: Dry 050402a. lms					
SetA	skir:781:-Z	skir781-Z1			
		skir781-Z2			
	skir:782:-Y	skir782-Y1	050402	1820	
		skir782-Y2			red tip (do not use amp for freq)
Project: ModImpact Dry 050402a. lms					
	skir:782:-Y	skir782-Y1			
		skir782-Y2	050402	1834	red tip (do not use amp for freq)
Move Accel to SetB					
Project: ModImpact Dry 050402b. lms					
SetB	skir:782:-Y	skir782-Y1	050402	2247	
		skir782-Y2			
	hda:182:-X	hda:182:-X1		2324	
	skir:781:-X	skir:781:-X1			
	ring:481:+Y	ring:481:+Y1			
	ring:484:-Z	ring:484:-Z1			
	hdb:281:+X	hdb:281:+X1			
	ring:482:+X	ring:482:+X1			
	ring:483:-Z	ring:483:-Z1	050403	0027	
	hdb:281:-Y	hdb:281:-Y1			
	top:881:-Z	top:881:-Z1			

Data Collected By: SetA: Neilsen/DeBardeleben Signature: SetB: Sandstrom, Mehta, Thakkar

Verified By: SetA: Mehta SetB: Neilsen Signature:

Date Performed: 050402/050403

Test Equip., Serial No. & Calibration Due Date:

(3)

Data Log — Dryer Modal

(Section) Title of Test	Impact Hammer Location	(Run) Data Filename	Date and Time of Acquisition		Comments Gain Settings
Project: Mod Impact Dy		050403a. lms			
Set C	top: 881: -Z	top: 881: -Z1	050403	0533	
		top: 881: -Z2			
	Sidd: 681: -Y	Sidd: 681: -Y1			
	ring: 483: -Z	ring: 483: -Z1			
	ring: 482: -Z +X	ring: 482: +X1			
	hdb: 281: +X	hdb: 281: +X1			
	ring: 484: -Z	ring: 484: -Z1			
	ring: 481: +Y	ring: 481: +Y1			
	hdb: 182: -X	hdb: 182: -X1			
	skir: 781: -X	skir: 781: -X1			
	skir: 782: -Y	skir: 782: -Y1	050403	0715	
	Move to Set D (Some of same points as Set C)				
Project: Mod Impact Dy		050403b. lms			
Set D	skir: 782: -Y	skir: 782: -Y2	050403	0919	
	skir: 781: -X	skir: 782: -Y2			
	skir: 781: -X	skir: 781: -X1			
	hda: 182: -X	hda: 182: -X1			
	ring: 481: +Y	ring: 481: +Y1	050403	1031	
	ring: 484: -Z	ring: 484: -Z1			
	hdb: 281: +X	hdb: 281: +X1			
	ring: 482: +X	ring 482 +X1			
	ring: 483: -Z	ring 483 -Z1			
	sidd: 681: -Y	Sidd 681: -Y1			
	top: 881: -Z	top: 881: -Z1	050403	1129	

Set C: Sandstrom / Melitz

Data Collected By: Set D: De Bra banderes / Neiheisel Signature: [signatures]

Verified By: Set C: Neiheisel Set D Melitz Signature: Set C: [signature] Set D: [signature]

Date Performed: 050403

Test Equip., Serial No. & Calibration Due Date:

(4)

Data Log Dryer Modal

Note: Saved over by below

Title of Test (Section)	Impact Hammer Location	Data Filename (Run)	Date and Time of Acquisition	~~Gain Settings~~ Comments
Project: ModImp Dry050403 SetE.lms (On Desktop PC)				
	Freq. Domain			
SetE	skir:781:-X	skir781-X1	050403 1305	
	skir:783:-X	skir783-X1		
		skir783-X2		Investigate windowing, Remove windows
	skir:784:-X	skir784-X1		
		skir784-X2		red tip hid or stra
	skir:785:-X	skir785-X1		gray tip
	skir:786:+X	skir786+X1		
	skir:787:+X	skir787+X1	050403 1340 ~~1630~~	
Project: Dry050403 SetE.lms			mislabelled – actually labelled as ModImpDry050403SetE.lms and saved over above	
	Time Domain			
SetE	skir:787:+X	skir787+X1	050403 1352	
		skir787+X2		
	skir:786:+X	skir786+X1		
		skir786+X2		
	skir:785:-X	skir785-X1		
		skir785-X2		
	skir:784:~~+X~~-X	skir784-X1		
		skir784-X2		
	skir:783:-X	skir783-X1		
		skir783-X2	050403 1420	
	Fill to LWL			

Data Collected By: De Brabandere / Neiheisel Signature: [signatures]

Verified By: Melitz Signature: [signature]

Date Performed: 050403

Test Equip., Serial No. & Calibration Due Date:

(5)

Data Log — Dryer Modal

(Section) Title of Test	Impact Hammer Location	(Run) Data Filename	Date and Time of Acquisition		Comments Gain Settings
Project: SpecAcqL		W050403SctE.lvm			
SctE	Skir:756:+X		050403	1635	
	Skir:787:+X				
	Skir:783:-X				
	Skir:785:-X				
	Skir:784:-X				
			050403	1657	
Project: ModImpLW050403SctE.lvm					
SctE	Skir:784:-X	Skir:784:-X1	050403	1707	
	Skir:783:-X	Skir:783:-X1			
	Skir:785:-X	Skir:785:-X1			
	Skir:781:-X	Skir:781:-X1			
	Skir:786:+X	Skir:786:+X1			
	Skir:787:+X	Skir:787:+X1	050403	1734	

Data Collected By: De Brabandere / Neiheisel Signature: D Brabandere M Neiheisel

Verified By: Meltz Signature:

Date Performed: 050403

Test Equip., Serial No. & Calibration Due Date:

(6)

Data Log — Dryer Modal

(Section) Title of Test	Impact Hammer Location	(Run) Data Filename	Date and Time of Acquisition		Comments Gain Settings
Project: ModImpMWL 050403 SetD.lms					
Set-D	ring:483:-Z	ring:483:-Z1	050403	2056	
	ring:482:+X	ring:482:+X1			
	hdb:281:+X	hdb:281:+X1			
	ring:481:+Y	ring:481:+Y1			
	ring:484:-Z	ring:484:-Z1			
	hda:182:-X	hda:182:-X1			
	skir:781:-X	skir:781:-X1			
	skir:782:-Y	skir:782:-Y1			
	sidd:681:-Y	sidd:681:-Y1			
	top:881:-Z	top:881:-Z1	050403	2232	
Project: ModImpMWL 050403 SetD.lms					
Set-D	top:881:-Z	top:881:-Z1	050403	2309	
	sidd:681:-Y	sidd:681:-Y1			
	skir:782:-Y	skir:782:-Y1			
	skir:781:-X	skir:781:-X1			
	hda:182:-X	hda:182:-X1			
	ring:481:+Y	ring:481:+Y1			
	hdb:281:+X	hdb:281:+X1			
	ring:482:+X	ring:482:+X1			
		ring:482:+X2			
	ring:483:-Z	ring:483:-Z1			
	ring:484:-Z	ring:484:-Z1	050404	0024	
Project: ModImpMWL 050404 SetE.lms					
	skir:784:-X	skir:784:-X1	050404	0104	
	skir:783:-X	skir:783:-X1			
	skir:785:-X	skir:785:-X1			
	skir:781:-X	skir:781:-X1			
	skir:786:+X	skir:786:+X1			
	skir:787:+X	skir:787:+X1	050404	0133	

Data Collected By: Meitz / Sandstrom — Signature: Alex Sandstrom

Verified By: Nezhiesel — Signature: Michael T Nezhiesel

Date Performed: 050403 / 050404

Test Equip., Serial No. & Calibration Due Date:

(7)

Data Log — Dryer Modal

(Section) Title of Test	Impact Hammer Location	(Run) Data Filename	Date and Time of Acquisition		Comments Gain Settings
Project: ~~Mod Emp~~ Spec Acq MWL 050404 SetE.lms					
SetE	Skir:781:-X	Skir:781:-X1	050404	0143	
		Skir:781:-X2			
	Skir:785:-X	Skir:785:-X1			
		Skir:785:-X2			
	Skin:784:-X	Skir:784:-X1			
		" " 2			
		" " 3			
		" " 4			
		" " 5			
	Skir:783:-X	Skir:783:-X1			
		" " 2			
	Skir:787:+X	Skir:787:+X1			
		Skir:787:+X2			
	Skir:786:+X	Skir:786:+X1			
		Skir:786:+X2	050404	0201	
Project: Spec Acq MWL 050404 SetE.lms					
SetE	Skir:786:+X	Skir:786:+X1	050404	0312	
		" " 2			
	Skir:787:+X	Skir:787:+X1			
		Skir:787:+X2			
	Skir:783:-X	Skir:783:-X1			
		" " 2			
	Skir:784:-X	Skir:784:-X1			
		" " 2			
		" " 3			
	Skir:785:-X	Skir:785:-X1			
		Skir:785:-X2			
	Skir:781:-X	Skir:781:-X1			
		" " 2	050404	0328	

Data Collected By: Melitz/Sandstrom Signature: Eugene Melitz

Verified By: Neiheisel Signature: Mark T. Neiheisel

Date Performed: 050404

Test Equip., Serial No. & Calibration Due Date:

(8)

Data Log — Dryer Modal

(Section) (Run)

Title of Test	Impact Hammer Location	Data Filename	Date and Time of Acquisition	Gain Settings	Comments
Project: ModImp HWL 050404 SetE. lms					
SetE	Skir:781:-X	Skir:781:-X1	050404 0336		
	Skir:785:-X	Skir:785:-X1			
	Skir:784:-X	Skir:784:-X1			
	Skir:783:-X	Skir:783:-X1			
	Skir:786-787:+X	Skir:787:+X1			
	Skir:786:+X	Skir:786:+X1	050404 0400		
Project: SpecAcq ModImp HWL 050404 SetD. lms					
SetD	ring:483:-Z	ring:483:-Z1	050404 0429		
		" " " 2			
	ring:482:+X	ring:482:+X1			
	hdb:281:+X	hdb:281:+X1			
	ring:484:-Z	ring:484:-Z1			
	ring:481:+Y	ring:481:+Y1			
	hda:182:-X	hda:182:-X1			
	Skir:781:-X	Skir:781:-X1			
	skir:782:-Y	skir:782:-Y1			
	sidd:681:-Y	sidd:681:-Y1			
	top:881:-Z	top:881:-Z1	050404 0542		
Project: ModImp HWL 050404 SetB. lms					
SetB	top:881:-Z	top:881:-Z1	050404 1010		
	sidd:681:+X	sidd:681:+X1			
	skir:782:-Y	skir:782:-Y1			
	Skir:781:-X	Skir:781:-X1			
	hda:182:-X	hda:182:-X1			
		" " " 2			
	ring:481:+Y	ring:481:+Y1			
	ring:484:-Z	ring:484:-Z1			
	hdb:281:+X	hdb:281:+X1			
	ring:482:+X	ring:482:+X1			
	ring:483:-Z	ring:483:-Z1	050404 1253		

SetE/D Melitz/Sanderson SetE/D Ben

Data Collected By: SetB Neiheisel/DeBrabander Signature: SetB Michael P. Neiheisel DB

SetE/D Neiheisel

Verified By: SetB Melitz Signature:

Date Performed: 050404

Test Equip., Serial No. & Calibration Due Date:

(9)

Data Log — Dryer Modal

(Section) (Pin) Comment

Title of Test	Impact Hammer Location	Data Filename	Date and Time of Acquisition	Gain Settings
Project: ModImpMkII		050404Set B.lms		
Set-B_MM	ring:483:-Z	ring:483:-Z1	050404 1424	
	ring:482:+X	ring:482:+X1		
	hdb:281:+X	hdb:281:+X1		
	ring:484:-Z	ring:484:-Z1		
	ring:481:+Y	ring:481:+Y1		
	hda:182:-X	hda:182:-X1		
	skir:781:-X	skir:781:-X1		
	skir:782:-Y	skir:782:-Y1		
	sidd:681:-Y	sidd:681:-Y1		
	top:881:-Z	top:881:-Z1	050404 1540	
Project: ModImpLWL		050404 Set-B.lms		
Set-B_LWL	top:881:-Z	top:881:-Z1	050404 1631	
	sidd:681:-Y	sidd:681:-Y1		
	skir:782:-Y	skir:782:-Y1		
	skir:781:-X	skir:781:-X1		
	hda:182:-X	hda:182:-X1		
	ring:481:-Y	ring:481:-Y1		
	ring:484:-Z	ring:484:-Z1		
	hdb:281:+X	hdb:281:+X1		
	ring:482:+X	ring:482:+X1		
	ring:483:-Z	ring:483:-Z1	050404 1930	
Dryer Moved for laser dimensional measurements				

Data Collected By: Neiheisel/De Brabandere Signature:

Verified By: Meltz Signature:

Date Performed: 050404

Test Equip., Serial No. & Calibration Due Date:

(10)

Data Log — Dryer Modal

(Run) Section — Comments

Title of Test	Impact Hammer Location	Data Filename	Date and Time of Acquisition	Gain Settings
Project: ModImpLWL050406 SetA.lms				
SetA-HWL	skir:781:-X	sk.r:781:-X1		
	skir:783:-X	sk.r:783:-X1		
	skir:782:-X	skir:782:-X1		
	ring:484:-Z	ring:484:-Z1		
	ring:483:-Y	ring:483:-Y1		
	ldb:281:+X	ldb:281:+X1		
	ring:482:+X	ring:482:+X1		
	ring:483:-Z	ring:483:-Z1		
	sidd:681:-Y	sidd:681:-Y1		
	top:681:881:-Z	top:881:-Z1		
		top:881:-Z 0.25Hz1		switch to 0.25Hz LP
		top:881:-Z 0.5Hz1		switch to 0.5Hz LP
		top:881:-Z 1Hz1		switch to 1Hz LP
Project: ModImpHWL050406 SetA.lms				
	top:881:-Z	top:881:-Z1		
	sidd:681:-Y	sidd:681:-Y1		
	ring:482:+X	ring:482:+X1		
	ring:483:-Z	ring:483:-Z1		
	ldb:281:+X	ldb:281:+X1		
	ring:481:+Y	ring:481:+Y1		
	ring:484:-Z	ring:484:-Z1		
	ldd:182:-X	ldd:182:-X1		
	skir:783:-X	sk.r:783:-X1		
		skir:783:-X for Damping		
	skir:781:-X	skir:781:-X1		
		skir:781:-X for Damping		
	skir:782:-Y	sk.r:782:-Y for Damping		
Project: ModImpLWL050406 SetA.lms				
	ldd:182:-X	ldd:182:-X1		

Data Collected By: Falbo/Nesheiwat Signature: [signature]

Verified By: DeBrabandere Signature: [signature]

Date Performed: 050406

Test Equip., Serial No. & Calibration Due Date:

(11)

Data Log — Dryer Modal / Static Load

(Section) Static Load (Run)

Title of Test	Impact Hammer Location	Data Filename	Date and Time of Acquisition	Gain Settings	Comments
	Project: Static Load 050406a.lms				
Static Load		Run 1	050406 2352		
		Run 2			No Good
		Run 3			
		Run 4	050407 0029	Support	Weld Broke at end. No Through Put

Data Collected By: De Brabander Signature: De Brabander

Verified By: Netherclift Signature: Netherclift

Date Performed: 050406/050407

Test Equip., Serial No. & Calibration Due Date:

(12)

Data Log — Dryer Modal

(Set) (Run)

Title of Test	Impact Hammer Location	Data Filename	Date and Time of Acquisition	Gain Settings
Project: Mod Impact LWL	050407a	Set C	~~050407~~ ~~0220~~	
Set C low-LW	hda:182:-X	hda:182:-X1	050407 0220	
	skir:781:-X	skir:781:-X1		
	skir:782:-Y	skir:782:-Y1		
	sidd:681:-Y	sidd:681:-Y1		
	top:881:-Z	top:881:-Z1		
	skir:783:-X	skir:783:-X1		
	ring:481:+Y	ring:481:+Y1		
	ring:484:-Z	ring:484:-Z1		
	hda:281:+X	hda:281:+X1		
	ring:482:~~-Z~~ +X	ring:482:+X1		
	ring:483:-Z	ring:483:-Z1	050407 0429	

Data Collected By: Melitz/De Brabandere Signature: D Brabandere

Verified By: Nelsel Signature:

Date Performed: 050406/050407

Test Equip., Serial No. & Calibration Due Date: